This is a peer-reviewed, accepted author manuscript of the following research article: Theotokatos, G., Rentizelas, A., Guan, C., & Ancic, I. (Accepted/In press). Waste heat recovery steam systems techno-economic and environmental investigation for ocean-going vessels considering actual operating profiles. *Journal of Cleaner Production*

Waste heat recovery steam systems techno-economic and environmental investigation for ocean-going vessels considering actual operating profiles

Gerasimos Theotokatos[1*], Athanasios Rentizelas[2], Cong Guan[3] and Ivica Ancic[1]

1 Maritime Safety Research Centre, Department of Naval Architecture, Ocean and Marine Engineering, University of Strathclyde, 100 Montrose Street, Glasgow, G4 0LZ, Scotland, UK

2 School of Mechanical Engineering Management, National Technical University of Athens, 9 Iroon Polytechneiou, Zografou, GR15780, Greece

3 Key Laboratory of High Performance Ship Technology of Ministry of Education, School of Energy and Power Engineering, Wuhan University of Technology, Wuhan, China

* Corresponding author

Abstract

Waste heat recovery steam systems is a proven technology for improving the ship power plant efficiency and reducing the ship environmental footprint, thus their usage can respond to the pressure for decarbonising the shipping operations. This study aims at investigating the techno-economic feasibility of various waste heat recovery steam systems whilst assessing their environmental impact for three ocean-going tanker vessels with their type spanning from Handymax size to very large crude carriers. Thermodynamic modelling of the investigated systems is employed for estimating the systems performance parameters including the generated electric power and fuel savings taking into account the vessels actual operating profiles and typical annual voyages characteristics. The systems net present value and the profitability index indicators are employed for assessing the systems economic feasibility, whereas the systems environmental impact is evaluated by using the achieved annual carbon dioxide emissions reduction. Two different nominal turbo-generator sizes matching the ship main engine full-load and part-load conditions are investigated, whereas a sensitivity analysis on the fuels prices is carried out to identify the marginal fuel price that renders the investment of each investigated system profitable. The derived results demonstrate that the single pressure waste heat recovery system sized for the ship engine part-load operation provides an attractive solution depending on the vessel type considering the technical, economic and environmental parameters. This study results in better insights on the impacts of the investigated energy efficiency improvement technologies for tanker ships, thus it can prove useful support for designing future sustainable ship power plants.

Key words Waste Heat Recovery steam systems; techno-economic and environmental feasibility; actual operating profiles; full and part-load design; ocean-going vessels; marginal fuel price.

Highlights

- Dual pressure waste heat recovery steam system analysis using a thermodynamic model
- Techno-economic-environmental assessment of waste heat recovery steam systems
- Three tankers actual operating profiles and systems design at full/part-load conditions
- Marginal HFO prices determined for identifying profitable investments
- Part-load sized single pressure system is feasible considering all parameters

Nomenclature list

Abbreviations

AC	alternating current
AE	auxiliary engine
BSFC	brake specific fuel consumption
ECA	emission control area
EEDI	Energy Efficiency Design Index
E/G	exhaust gas
FC	fuel consumption
FW	feed water
HFO	heavy fuel oil
HP	high pressure
HT	high temperature
IMO	International Maritime Organization
LO	lubricating oil
LP	low pressure
MCR	maximum continuous rating
MGO	marine gas oil
ORC	Organic Rankine Cycle
ST	steam turbine
SW	sea water
VLCC	very large crude carrier
WHR	waste heat recovery
WHR1	single pressure WHR steam system
WHR2	dual pressure WHR steam system

Symbols

a	power exponent (-)
$BSFS$	brake specific fuel onsimption (g/kWh)
c	power coefficient (-)
c_p	specific heat capacity at constant pressure (kJ/kgK)
$CAPEX$	Capital Expenditure (€)
dr	real discount rate (−)
$ECO2$	CO_2 emissions reduction (kg)
EF	emissions factor (g CO_2/g fuel)
f	correction factor (−)
FS	fuel savings (kg)
h	specific enthalpy (kJ/kg)
H_L	fuel lower heating value (kJ/kg)
L	load (−)
$\dot{m}$	mass flow rate (kg/s)
n	economic lifetime of investment (years)
NPV	Net Present Value (€)
$OPEX$	Operational Expenditure (€/year)
p	pressure (Pa)
P	power (kW)
PI	Profitability Index (−)
$\dot{Q}$	thermal power (kW)
r	ratio (−)
S	Savings (€/year)
t	operating time (h)
T	temperature (°C)
v	ship speed (knots)

Greek symbols

η	efficiency (-)
ρ	mass density (kg/m^3)

Subscripts

a	air
AC	alternating current
AB	auxiliary boiler
AE	auxiliary engine
ac	air cooler
b	boiler/back pressure
c	condenser
d	downstream
e	engine
ec	economiser
el	electric
ev	evaporator
f	fuel
fw	feed water
g	gas
gen	generator
hfw	heating feed water
hs	ship heating service
HP	high pressure
is	isentropic
jwc	jacket water cooler
mech	mechanical
o	outlet
pp	pinch point
s	steam
sh	superheater
st	steam turbine
sw	sea water
T	temperature

.

127	tg	Turbo-generator	129	w	water
128	u	upstream	130	WHR	waste heat recovery

1. Introduction

The existing and forthcoming stringent environmental regulations have increased the pressure to the maritime industry for decarbonising shipping operations. Specifically, the International Maritime Organisation (IMO) introduced the energy efficiency design index (EEDI) regulations (IMO, 2014), requiring the gradual reduction of the CO_2 emissions up to 30% by 2025 compared to the baseline levels corresponding to 2013-2014 ship designs . In addition, the Paris agreement was adopted by the IMO implying that initiatives to reduce CO_2 emissions by 50% by 2050 need to be pursued (IMO, 2018). Considering the imposed regulations on other greenhouse and non-greenhouse pollutants, the fuel prices volatility, the need for the shipping companies viability, the societal needs as well as the shipping sector international character, the enhancement of the shipping operations sustainability becomes a quintessential task. In this respect, a number of previous studies assessed potential technologies and systems considering all sustainability aspects (economic, environmental, social) (Basurko and Mesbahi, 2014; Bolbot et al., 2020; Iannaccone et al., 2020). The environmental-economic feasibility of various propulsion plant alternatives were assessed in Trivyza et al. (2018), whereas the influence of alternative fuels were elaborated in Brynolf et al. (2014) and Gilbert et al. (2018). Emission abatement technologies and systems are analysed in Bouman et al. (2017), Makkonen and Inkinen (2018), and Schwartz et al. (2020). Siu Lee Lam and Lai (2015) elaborated the environmental sustainability enhancement of shipping operations. Effective design and operational measures for improving the shipping operations efficiency and reducing the operational expenditure are discussed in Trivyza et al. (2018) and Dere and Deniz (2019). Design measures typically include energy saving devices for the ship hull and propeller, improved hull and propeller designs, wind assisting propulsion, control of electric motors speed via frequency converters, use of alternative fuels of low carbon content and waste heat recovery (WHR) systems.

Considering that typically 50% of the fuel energy in marine engines is wasted, while the engine exhaust gas wasted energy amounts to around 25% of the fuel energy, WHR systems are a prominent solution to improve the power plant efficiency (Theotokatos and Livanos, 2013). Hence, WHR systems employing as working medium either water/steam or organic fluids have been proposed for covering the ship thermal and/or electric energy demand (Larsen et al. 2014).

Various systems that recover heat from the engine exhaust gas were analysed in the pertinent literature. These include the simpler exhaust gas economiser (for producing saturated steam that covers the ship heating services)

or the more complex single pressure or dual pressure steam systems for producing both saturated and superheated steam. The exhaust gas use is the most common alternative (Ma et al., 2012; Larsen et al., 2013; Yang et al., 2013) that is typically considered as the baseline (MAN, 2012; MAN, 2014). WHR systems of this type can be installed on new ships or retrofits (Altosole et al., 2014). Additionally, the charge air cooler use for pre-heating the feed water can be employed to increase the wasted heat recovered amount (Grimmelius et al., 2010; Hountalas et al., 2012). The dual pressure steam system configurations are quite complex recovering heat from the engine exhaust gas via an exhaust gas boiler as well as the engine jacket water, air and lubricating oil coolers. Benvenuto et al. (2014) analysed this system type outlining its advantages and limitations for the low temperature heat conversion. For overcoming these limitations, Organic Rankine Cycle (ORC) systems have been introduced in the transportation (Pili et al., 2017) and maritime applications (Tzortzis and Frangopoulos, 2018, Uusitalo et al, 2019). Due to the organic fluids characteristics, the ORC systems can recover low quality heat, thus increasing the potential for electric power generation, effectively matching the thermal sources and the employed thermodynamic cycle, which can be optimised by appropriately selecting the working fluid (Yang and Yeh, 2014). Previous Studies on ORC systems marine applications analysed the potential to apply an ORC WHR system for marine diesel engines (Song et al. 2015), the combined use of thermo-electric generator (TEG) and ORC for marine engines (Zhang et al. 2015). Zhang et al. (2019) investigated the sustainability of the ORC system for power generation.

For increasing the recovered heat amount, systems that employ other wasted heat sources and media including the engine cooling water, scavenge air and lubricating oil have been analysed. Yang et al. (2014) analysed a dual loop ORC for marine engines operating at varying operating conditions. Dimopoulos et al. (2011) considerd four operational conditions for optimising a WHR steam system. Choi and Kim (2013) analysed a ship operating profile identifying two main conditions and optimised a dual-loop ORC system for those conditions. Kalikatzarakis and Frangopoulos (2014) took into account the full operating profile when optimising an ORC system and demonstrated that different profiles have a large impact on the system economic performance. Baldi et al. (2015) systematically investigated the influence of accounting for the ship operational profile for optimising the combined cycle design and operating variables. Depending on the ship operating profile, dual parallel ORC systems can be more effective (Yun et al., 2015). The system capital and installation costs become higher with increasing complexity whilst the generated electric power increases, thus improving the overall power plant efficiency, reducing the fuel consumption and the operational expenditure (Vittorini et al., 2019). This is particularly important for large ocean-going vessels profitability, which depends on various parameters including the ship route and

freight price (Wu and Huang, 2018).

In addition to increasing the power plants efficiency, the usage of the WHR systems on-board ocean-going vessels can contribute to the CO_2 emissions reduction (Balcombe et al., 2019). These vessels represent the 84.7% of the world fleet (UNCTAD, 2017) and typically operate at steady state conditions (manoeuvring includes less than 5% of their operational time), whereas their engine rooms are spacious enough to accommodate the WHR systems.

Comparing the WHR systems using steam and organic fluids, it is concluded that the steam systems are a mature technology, safely used for decades on-board ships. Safety issues related with the shipboard storage and usage of organic fluids were reported in Zhang et al. (2012), where appropriate technologies and measures are proposed to ensure these systems safe operation. However, the ship owners/operators are still sceptical on installing WHR systems to improve their ships energy efficiency (apart from exhaust gas economisers that are extensively used for producing saturated steam). In part, this is due to the lack of detailed and reliable techno-economic feasibility studies taking into account the design and operating characteristics of the ships power plants, as the majority of the previous studies focused on a very limited number of operating points (usually the main engine rated power). Thus, systematic studies are required to provide evidence and assess the feasibility and sustainability of the WHR systems alternatives.

From the preceding literature review, the following gaps were identified regarding the WHR applications for ship power plants: (a) the comparison of the WHR systems alternatives were carried out for only a small number of operating points, whilst the actual operating conditions and the engine actual operating profiles have not been extensively considered in studying the energy efficiency improvement; this resulted in over-estimating the actual benefits of the proposed WHR systems; (b) the ship size influence on the WHR systems performance has not been investigated as usually a specific engine is selected for studying the WHR system performance; (c) the WHR system components sizing and its effect on system techno-economic-environmental parameters have not been studied and; (d) the influence of the fuel prices variation considering actual operating profiles has not been investigated.

In this respect, this is the first study aiming at investigating the WHR steam systems technical, economic and environmental performance considering three tanker vessels of different sizes, their actual operating profiles, a number of WHR systems alternatives with their components being sized to match the ships engines full and part load conditions as well as the fuel prices variation. Thermodynamic modelling is employed along with the

economic and environmental parameters calculations. The derived results are analysed for simultaneously assessing the techno-economic and environmental impact of the investigated technologies identifying the most feasible alternatives, whilst evaluating the ship and the systems components size influence. Hence, this study provides decision support for designing sustainable ship power plants. This study novelty stems from the combination of state-of-the-art methods including thermodynamic modelling and economic analysis to systematically study the impact of the installation of WHR steam systems on the sustainability of the ship power plants and provide a better understanding of the underlying parameters that influence the technical, economic and environmental performance of these systems.

The remaining of this study is structured as follows. Section 2 describes the followed methodological steps. Section 3 describes the tanker power plant as well as the investigated WHR systems alternatives. Section 4 includes the WHR systems modelling along with the financial and environmental parameters calculations. The investigated case studies are described in Section 5. Section 6 includes the derived results and their discussion. Finally, the conclusions and main findings are summarized in Section 7.

2. Methodology

This study investigates the techno-economic and environmental impact of two WHR steam systems (of single pressure and double pressure type) for three tanker ships of different sizes. The methodology consists of five steps, which are described below. The flowchart of this methodology along with the involved steps interconnections is illustrated in Fig. 1.

- Step 1 consists of the collection of the investigated WHR and ship systems characteristics.
- Step 2 includes the thermodynamic modelling of the investigated WHR systems along with the models set up and validation.
- Step 3 consists of calculating the fuels and lubricating oil savings as well as the CO_2 emissions reduction.
- Step 4 consists of the systems economic analysis, the sensitivity analysis for the fuel prices and the calculation of the marginal prices that render the WHR systems profitable.
- Finally, Step 5 includes the results comparative analysis and discussion for assessing the techno-economic and environmental impact of the investigated systems as well as the influence of the ship size and the WHR systems components sizing.

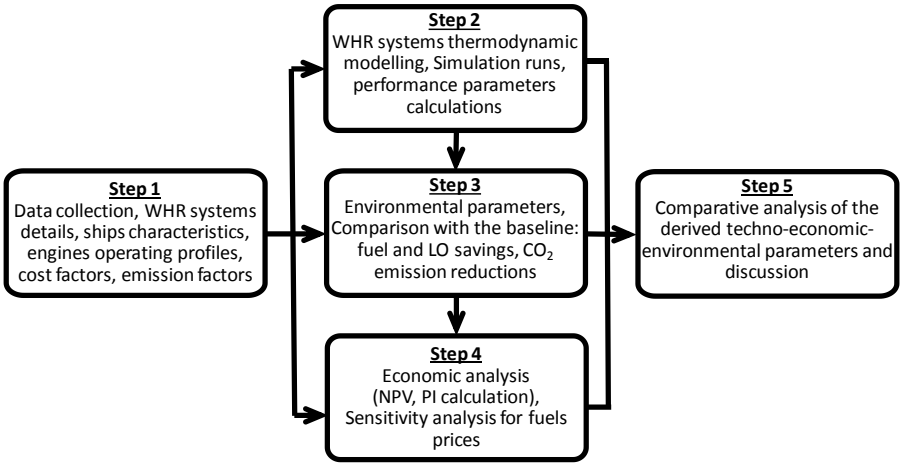

Figure 1. Flowchart of the methodology

3. Systems Description

3.1 Tankers vessels power plant

The smaller size tanker ships transport distilleries products that do not require heating, whereas the larger vessels transport crude oil, which requires heating during the voyage and unloading phases. In this respect, the voyage characteristics vary based on the vessel size. The smaller vessels (product carriers) tend to sail in shorter voyages but with more port calls, whereas the larger vessels typically trade between two locations (loading and destination ports) as reported in Burel et al. (2013), where the sailing time percentages spent within Environment Control Areas (ECA) various ship types are provided.

The ocean-going ships typically use conventional power systems; marine two stroke engines for propulsion directly coupled to the ship propeller, whilst the ship electric power is generated by diesel-generator sets (typically two to four) (Ancic et al., 2018). For product carriers, the thermal energy demand is typically covered by saturated steam produced either by the exhaust gas economiser (recovering thermal energy from the main engine exhaust gas) or an oil-fired auxiliary boiler. For crude carriers, typically two oil fired steam boilers are installed for covering the cargo thermal power demand, additionally to the auxiliary boiler that usually covers the other ship heating services demand (fuel heating, accommodation heating, etc.).

The ship propulsion (mechanical) energy demand corresponds to approximately 85% of the total ship energy (Dimopoulos et al., 2011; Trivyza et al., 2018.). One generator-set usually operates when the ship sails (under laden and ballast conditions), whilst two generator-sets typically operate when the ship manoeuvres or stays at port. Thus, the installation of a WHR system only for the main engine exhaust gas is usually targeted.

.

3.2 Investigated WHR steam systems

In this study, two WHR steam installations are investigated, in specific, the single pressure system (WHR1) and the dual pressure system (WHR2). The single pressure system schematic diagram is presented in Fig. 2. The system exhaust gas (E/G) boiler consists of three stages (economiser (or preheater), evaporator and superheater). The remaining system components include the water/steam drum, the turbo-generator, the feed water tank, the condenser, the system pumps (feed water pump, economiser circulating pump, evaporator circulating pump, condensate pump) and the external heat exchanger. For avoiding low temperature levels in the boiler exhaust gas outlet section, the temperature of the steam entering the economiser must be above 130ºC. This is obtained by the installation of the heat exchanger; alternative designs may include a three-way mixing valve, which however require a control system. The system provides the required saturated steam for covering the ship heating services demand and additionally generates electric energy, which covers a part of the ship demand for electricity.

The investigated dual pressure WHR steam system is schematically shown in Fig. 3. This system contains two steam drums (low pressure (LP) and high pressure (HP)) and an E/G boiler with five sections (LP evaporator, HP economiser, LP superheater, HP evaporator and HP superheater). For avoiding corrosion of the E/G boiler outlet components due to sulphuric acid condensation in the boiler outlet section (low temperature corrosion), the boiler does not include a LP economiser. The required supplementary waste heat recovery sources for preheating the feed water comes from the marine engine jacket cooler and the high temperature stage of the engine air cooler. A part of the HP saturated steam is utilized for the ship heating services, whereas the superheated steam (both LP and HP) expands in the steam turbine (consisting of two pressure stages) that drives the electric generator.

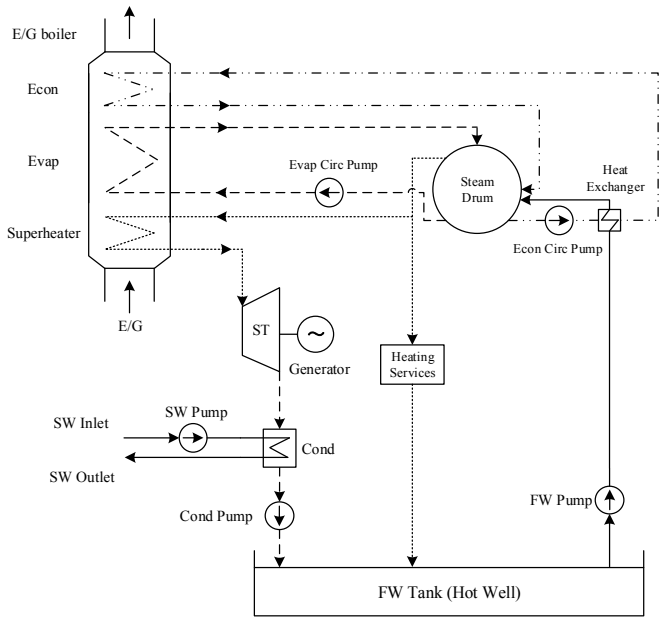

Figure 2. Schematic diagram of the investigated single pressure WHR steam system (WHR1)

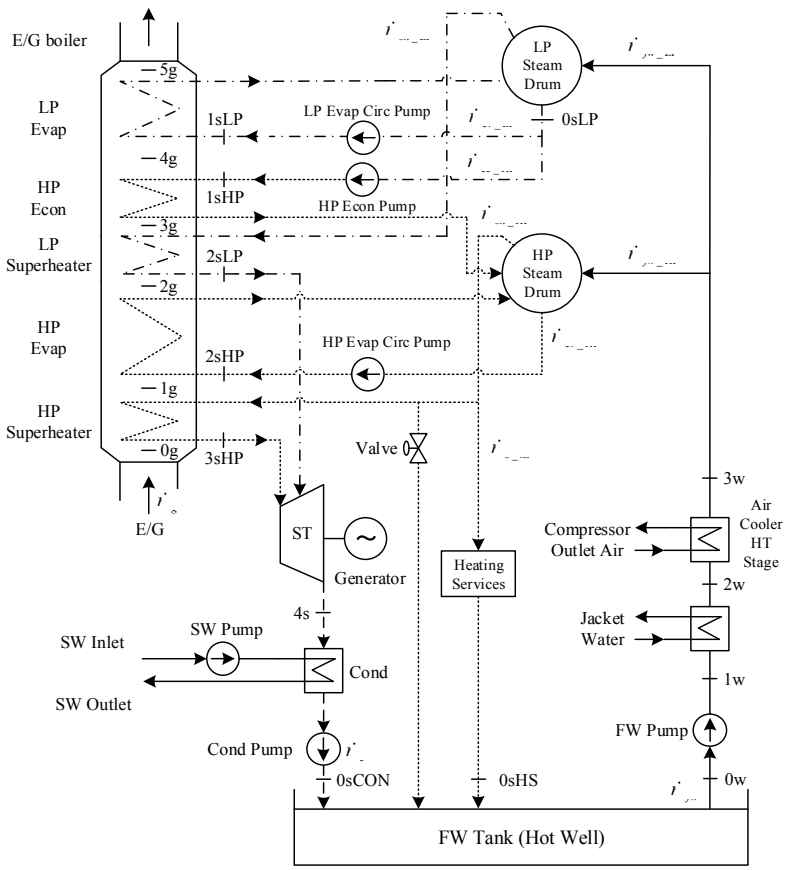

Figure 3. Schematic diagram of the investigated dual pressure WHR system steam (WHR2). HP: high pressure; LP: low pressure; SW: sea water; FW: feed water; HT: high temperature; ST: steam turbine. Evap: evaporator; Econ: economiser; Circ: circulating; Cond: condenser.

4. Calculations

4.1 WHR systems thermodynamic modelling

For modelling both the WHR systems, the continuity and energy conservation equations were applied for each system component considering the system operation at steady state conditions. Thermal losses were taken into account for the boiler and the heat exchangers via these components efficiencies, whereas pressure losses were taken into account for the piping sections including their fittings. The pumps required power was estimated based on the pump flow rate, pressure increase and efficiency. The efficiencies of the turbo-generator components (turbine, electric generator and mechanical connection) were also considered by using the data reported by SNAME (1990). The derived equations were manipulated to provide the equations for the calculation of the system working media mass flow rates. Subsequently, the thermal power of the system components and the generated electric power are calculated by using an iterative process.

The employed equations along with the used assumptions, the required input parameters as well as the

.

followed calculation procedure for the single pressure WHR steam system (WHR1) are described in Livanos et al. (2014) and therefore, they are not repeated herein. The calculation procedure for the dual pressure WHR steam system (WHR2) is described in the Appendix A. Both models were implemented in the MATLAB computational environment.

The WHR1 model was firstly introduced in Livanos et al. (2014) and it was validated by comparing the generated electric power for various engines using published manufacturers' data. Considering the same operating conditions, the model provided adequate accuracy, as it is reported in Livanos et al. (2014). The WHR2 model was validated by considering the percentage increase of the generated electric power from the WHR1 system respective values. This percentage increase was found to be in alignment with the data provided by the system manufacturer (MAN Diesel & Turbo, 2014; DSMS, 2008). It must be noted that the WHR systems realistic operation was investigated in this study, and hence, the derived predictions are more conservative compared with respective manufacturer data, for example, from MAN Diesel & Turbo (2014).

4.2 Fuel Savings and environmental parameters calculations

The fuel and lubricating oil savings are calculated by considering the operation of the ship power plant with the WHR systems in comparison with the respective baseline plant. This does not include a WHR system, assuming that the ship heating services are fully covered by using saturated steam generated from the vessels' auxiliary boiler. The ships laden and ballast sailing phases were considered, each phase consisting of sailing inside and outside ECAs by using Marine Gas Oil (MGO) and Heavy Fuel Oi (HFO), respectively. The ships engine operating profiles (operating time versus engine load) in the laden and ballast sailing phases are provided as input for the calculations. The generated electric power and saturated steam from the WHR systems reduces the operating time and fuel consumption of the ship auxiliary engines and boiler. The ship auxiliary engines operating time reduction also corresponds to lubricating oil savings. The WHR systems generated power is calculated by the employed models (described in Section 4.1) and depends on the ship main engine power (or load). It is assumed that there is an engine power threshold below that the WHR systems are switched off. For each fuel (HFO or MGO), the respective fuel saving (*FS* in kg) are calculated by using the following equation:

$$FS_f = \sum_m \sum_i \left(t_{m,i,f} P_{el,WHR} \frac{BSFC_{AE,f}}{1000} \right) - \sum_j \frac{t_{j,f} \dot{r}_{\ldots}}{\eta_{\mathrm{AB}} H_{L,f}} \quad (1)$$

where *f* denotes the fuel (HFO of MGO); *m* denotes the ship sailing mode (laden or ballast); *i* denotes the main engine operating point according to the respective operating profile; $t_{m,i,f}$ denotes the operating time (in h)

with the considered fuel for the m[th] sailing mode and the i[th] operating point of engine operating profile; $P_{el,WHR}$ (in kW) denotes the WHR system generated electric power (which depend on the main engine load); $BSFC_{AE,f}$ is the ship auxiliary engines brake specific fuel consumption for the considered fuel (in g/kWh), which for each fuel is calculated as $BSFC_{AE,ISO}H_{L,ISO} / H_{L,f}$; ISO denotes the ISO conditions;1000 corresponds to g/kg; $t_{j,f}$ denotes the operating time (in h) with the considered fuel in which the WHR system produces saturated steam flow rate $\dot{m}_{s,WHR,j}$ (in kg/h); Δh_s is the specific enthalpy difference for the steam evaporation; η_{AB} denotes the auxiliary boiler efficiency, and; $H_{L,f}$ (in kJ/kg) is the considered fuel lower heating value. The lubricating oil savings are calculated by using the first term of the right hand side of eq. (1) considering the LO specific consumption instead of the BSFC.

The fuel savings (for each fuel) of the different systems (in comparison to the baseline case) are also converted into CO_2 equivalent emission reductions by using the following equation:

$$ECO2 = EF_{HFO}FS_{HFO} + EF_{MGO}FS_{MGO} \quad (2)$$

The CO_2 emission factors for the HFO and MGO were taken as 3.114 g CO_2/g HFO and 3.206 g CO_2/g MGO, respectively (IMO, 2014). These emission factors values are estimated by considering the complete combustion chemical reactions taking into account a typical fuel composition, and they offer a sufficient approximation, as the incomplete combustion carbon pollutants amount is very small.

4.3 Economic analysis

For each investigated vessel and WHR system, investment analysis was performed to assess the yield of the additional investment required to install each system . This was done on a differential basis, meaning that only the differences in the system configuration and the respective operational, maintenance and investment costs or cost reductions/revenues compared to the baseline configuration were considered.

Each WHR system is considered as an investment, i.e. the capital expenditure (CAPEX) related to the equipment purchasing and installation. This initial investment would lead to a series of future cash flows, which have as revenue the expenditure reduction throughout the vessel lifetime due to the associated fuel savings and reduced lubricating oil consumption; the former is attributed to the increased power plant efficiency, whereas the latter to reduced operational time of the plant auxiliary engines. On the other hand, any operational costs that are specific to the WHR system are considered as expenses in the future cash flow calculations. These are primarily due to the WHR-specific maintenance required and it is assumed that the rest of the ship energy system is not

impacted in terms of operation and maintenance costs due to the WHR installation. The difference between the annual revenues and expenses determine the yearly cash flows of the investment. The future yearly cash flows are considered as a fixed annuity for the lifetime of the investment, since real values have been assumed.

In this study, two commonly used investment analysis indicators were employed: the Net Present Value (NPV) and the Profitability Index (PI). An investment with positive NPV is profitable, whereas a higher NPV denotes a higher return of investment in absolute terms. The NPV is a useful indicator to assess the economic performance of the various WHR technologies for the same vessel size. For each combination of WHR technology and vessel size, the NPV was calculated by the following equation:

$$NPV = \frac{CF}{dr}\left(1 - \frac{1}{(1+dr)^n}\right) - CAPEX_{WHR} \quad (3)$$

where *CF* is the yearly cash flow due to the addition of the WHR system. The real discount rate *dr* has been used in the discounting calculations of the annuity *CF* as the future cash flows have not been adjusted for inflation. CF is calculated according to the following equation:

$$CF = \mathrm{S_{HFO}} + S_{\mathrm{MGO}} + S_{LO} - OPEX \quad (4)$$

where S_{HFO}, S_{MGO}, S_{LO} are the savings from reduced consumption of HFO, MGO and Lubricating Oil respectively in €/year, and OPEX denotes the additional yearly operational expenditures due to the WHR system installation.

Since the capital expenditure for different vessel sizes can vary substantially, the NPV would not be an appropriate metric to compare the investments between different vessels. Therefore, the Profitability Index (PI) was used to this purpose, which is calculated as the ratio of the Present Value of the future cash flows, divided by the initial investment required, according to the following equation:

$$PI = \frac{NPV + CAPEX_{WHR}}{CAPEX_{WHR}} \quad (5)$$

The PI compares the future cash flows to the CAPEX and thus provides an indication of the profitability per invested capital unit. This allows for the fair comparison of the investments of different sizes (Rentizelas and Li, 2016). PI values greater than 1 indicate a profitable investment (a higher value denotes a more profitable investment per unit of capital expenditure). Both the NPV and PI indicators have been used for investment analysis in the energy sector as well as in shipping energy systems; example of the latter is provided in Qiu et al. (2019).

5. Case studies description

5.1 Investigated vessels characteristics

.

The selected tanker ships cover various sizes with their deadweight tonnage ranging from 55,000 to 280,000 t. The propulsion plant characteristics (required engine power and rotational speed) for these ships are reported in MAN (2013), whereas the engines brake specific fuel consumption (BSFC) was obtained from the engine manufacturer (MAN, 2019). It was assumed that the exhaust gas system back pressure is not affected by the WHR system, and therefore, pertinent corrections to BSFC were not applied. The saturated steam mass flow rates required for these ships heating needs were estimated from MAN (2012) and the respective steam balance calculations. The following values were considered for the saturated steam mass flows: 500 kg/h for the Handymax tanker, 1500 kg/h for the Suezmax tanker and, 1800 kg/h for the VLCC.

The investigated Suezmax tanker peak electricity demand during sailing is 780 kW. However, even in the case of operating the cargo pumps, shipboard measurements proved that the electricity power demand is lower than 935 kW (Grljusic et al, 2014). Based on the available measured data and the electric power balance calculations for the three investigated ships, the following average electric power demand values (in laden and ballast conditions) were assumed: 430 kW for the Handymax tanker; 700 kW for the Suezmax tanker and; 1000 kW for the VLCC. These ships diesel generators brake specific fuel consumption at the considered electric power was taken from their manufacturer data. The main characteristics of the ships and their propulsion plants including the installed auxiliary engines are provided in Table 1.

The exhaust gas temperature and mass flow rate for the three examined tankers propulsion engines, which were used in both the single and dual pressure WHR systems calculations, were taken from the respective manufacturer data (MAN, 2019) and are shown in Fig. 4. The exhaust gas temperatures for all the investigated cases are in the range of 230^{o}C−290^{o}C for the whole operating envelope. The exhaust gas temperature exhibits a minimum in the load range 75−85%, which is attributed to the selection of the engine settings for achieving the engine optimal efficiency in this load range. Higher engine efficiency implies lower exhaust gas wasted heat and lower exhaust gas temperature, which aligns with previous studies findings, for example, Guan et al. (2015). The exhaust gas mass flow rate and the thermal power (also presented in Fig. 4) depend on the engine power output and the engine size (thus, the ship size) and the considered engine operating point.

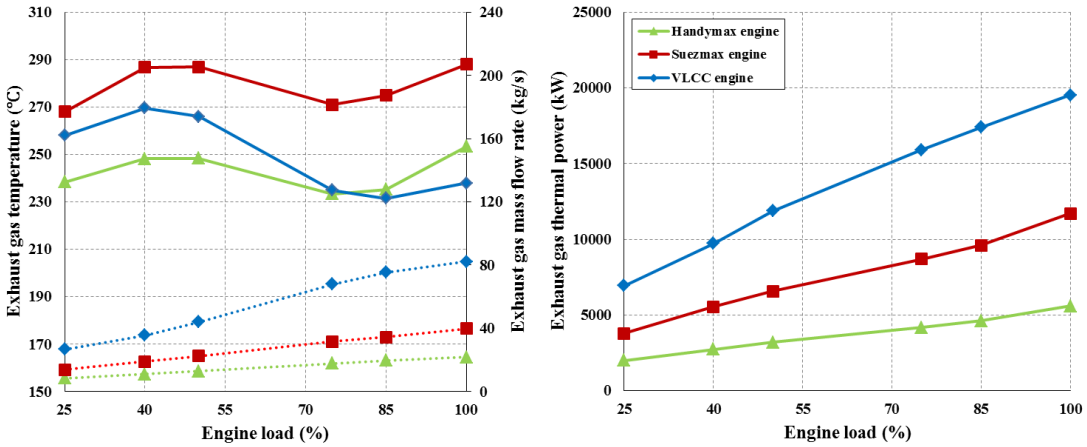

Figure 4. Investigated ships main engine exhaust gas parameters as a function of the engine load (in the left figure, the solid lines denote the temperature, whereas the dashed lines represent the mass flow rate).

5.2 WHR systems thermodynamic modelling input

The WHR2 model input parameters are listed in Table 2. The system components pressure losses and the employed temperature differences were taken from SNAME (1990). The water/steam properties were calculated by using the equations reported in Wagner and Kretzschmar (2008). The employed marine fuels were considered to consist of carbon, hydrogen and sulphur according to the typical values for HFO and MGO (IMO, 2008). The exhaust gas air/fuel equivalence ratio was used as input for estimating the exhaust gas composition considering complete combustion with excess air. The exhaust gas specific heat at constant pressure was calculated as function of the respective temperature and the exhaust gas composition (Heywood, 2018). The exhaust gas was assumed to consist of CO_2, H_2O, SO_2, O_2 and N_2, as the incomplete combustion products concentrations are small and therefore, thus not affecting the exhaust gas properties (Heywood, 2018).

Table 1. Main technical parameters of the investigated ships and engines.

Ship parameters			
Type	Handymax	Suezmax	VLCC
Ship size (dwt)	55000	160000	280000
Length overall (m)	183	274	333
Vessel speed (knot)	14.5	15	15.5
Main engine parameters			
Type	Two stroke	Two stroke	Two stroke
Bore (mm)	500	700	900
Brake power at MCR (kW)	7860	18780	31620
Engine speed at MCR (r/min)	129	95	78
BSFC at MCR (g/kWh)	179	176	173
Auxiliary engine parameters			
Average electricity load (kW)	430	700	1000
BSFC (g/kWh)	202	195	194

Heating services requirements			
Saturated steam for heating services (kg/h)	500	1500	1800

Table 2. Assumptions for the dual pressure WHR model calculation.

Parameter	Unit	Value
Boiler efficiency, η_b	%	99
Pressure of LP steam drum, p_{LP}	bar	4.8
Pressure of HP steam drum, p_{HP}	bar	8.0
Pressure of condenser, p_c	bar	0.065
Pressure of feed water tank, p_{fw}	bar	1.2
Pressure loss in the LP evaporator section, Δp_{ev_LP}	bar	15% p_{LP}
Pressure loss in the HP economiser section, Δp_{ec_HP}	bar	3% p_{HP}
Pressure loss in the LP superheater section, Δp_{sh_LP}	bar	5% p_{LP}
Pressure loss in the HP evaporator section, Δp_{ev_HP}	bar	15% p_{HP}
Pressure loss in the HP superheater section, Δp_{sh_HP}	bar	5% p_{HP}
Ratio of the LP evaporator circulating water to the produced LP saturated steam mass flow rates, r_{ev_LP}	-	3.0
Ratio of the HP economiser circulating water to the produced HP saturated steam mass flow rates, r_{ec_HP}	-	3.0
Ratio of the HP evaporator circulating water to the produced HP saturated steam mass flow rates, r_{ev_HP}	-	3.0
Ratio of the LP superheated steam to the HP superheated steam mass flow rates, r_{sh_LH}	-	0.3
Boiler inlet exhaust gas and outlet HP superheated steam temperature difference, T_{0g}-T_{3sHP}	°C	25
LP superheater inlet and outlet exhaust gas temperature difference, T_{2g}-T_{3g}	°C	10
Sulphuric acid dew point, T_{acid_dew}	°C	155

5.3 Operating profiles

The actual operational hours were assumed to be 7884 h per year considering that 10% of the total annual operating time is required for the ship maintenance (Guan et al., 2015). Laulajainen (2011) reported the voyage type characteristics for tankers of various sizes including Handymax and Suezmax concluding that the larger tankers tend to spend less operational time in ports as they undergo longer voyages. Due to unavailability of more recent data, the voyage distributions profiles for the Handymax and Suezmax tankers were estimated taking into account the average values for 2010 and 2011 reported in Banks et al. (2013). As data for the VLCC operating profile was not available, a voyage type distribution was assumed based on the Suezmax case with 5% less time staying in ports and 2.5% more time sailing in the laden and ballast modes. The different ships operational times within ECAs were estimated according to Burel et al. (2013). The investigated tankers voyage type distributions used in this study are presented in Table 3.

.

437 The speed profiles for the Handymax and Suezmax tankers were also derived by using the data reported in
438 Banks et al. (2013), where it was stated that the tankers speeds shifted from 2008 to 2011 towards lower ranges.
439 The average ship speeds profiles of the years 2010 and 2011 were considered herein for the estimation of the
440 vessels engine operating profiles, since this is the most recent data available. In addition, the VLCC speed profile
441 was assumed to be the same as the one of the Suezmax tanker (due to data unavailability and the similarities
442 between these two ship types voyage characteristics).

443 The engine power and the ship speed are connected by a power law (MAN, 2011) as represented by the
444 following equation:

445 $$P_e = cv^a \quad (6)$$

446 where P_e denotes the engine power in kW, v denotes the ship speed in knots, c denotes the power coefficient that
447 is taken as constant, and a denotes the power exponent with values from 3.5 to 4.5 depending on the ship type.
448 The investigated tankers propulsion engines operating profiles in laden and ballast conditions were estimated and
449 presented in Fig. 5 by employing eq. (6) and considering the ship speed profiles, 15% sea margin (to account for
450 varying weather conditions) and 12% margin to account for hull/propeller fouling. It can be inferred that the
451 Handymax tanker propulsion engine spends very limited time in loads above 65%, whereas other tankers
452 propulsion engines usually operate in a wider range of loads (from 25% to 100%).

453 **Table 3.** The voyage type distribution of the investigated ships.

	Handymax tanker	Suezmax tanker	VLCC
Theoretical operational hours (h/year)	8760	8760	8760
Maintenance time (%)	10	10	10
Actual operational hours (h/year)	7884	7884	7884
Time in laden (%)	31.4	34.0	36.5
Time in ballast (%)	12.9	28.9	31.5
Time in port (%)	55.7	37.1	32.0
Time in ECA (%)	50	20	20

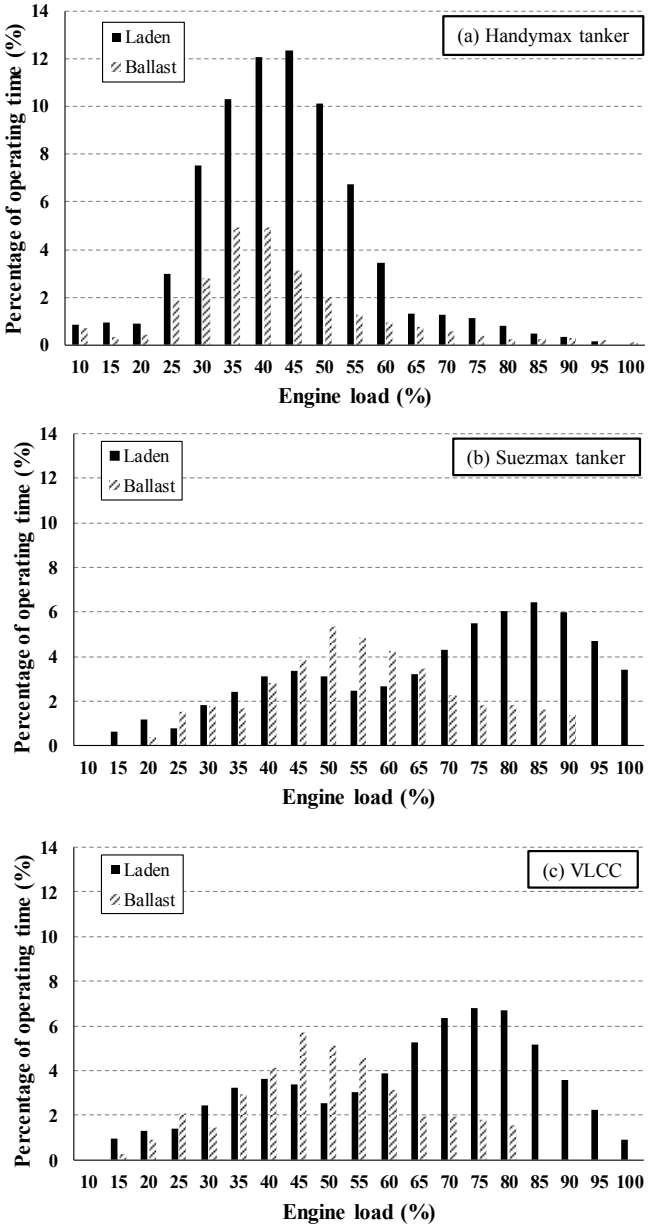

Figure 5. Investigated tankers engines operating profiles: (a) Handymax tanker; (b) Suezmax tanker; (c) VLCC.

5.4 Economic analysis input parameters

The input parameters for the economic analysis are presented in Table 4. All capital and operational costs apart from fuel costs are expressed on a 2015 year reference. The fuel costs are average values between 11/2014 and 11/2019. The WHR systems relative costs must be read along with the reference engines MCR power. The WHR1 system capital cost was obtained for an engine with 8.7 MW MCR power, whilst data for the WHR2 system was available for an engine with 29.3 MW MCR power. A scale factor of 0.75 was considered for the calculation of both WHR systems cost in other engine MCR powers. For estimating the CAPEX of the WHR systems with their turbo-generators sized at the engine part-load conditions, the turbo-generator cost and scale factor were used

464 according to the data reported in DOE (2016).

465 **Table 4.** Main economic parameters of the investigated ship system configurations.

Financial parameters	Value	Source/comments
Discount rate (real) (%)	12	Assumption
Service life (years)	25	Assumption, equal to expected ship service life
HFO cost (€/t)	369	Ship and bunker (2019), average Nov 2014 – Nov 2019
MGO cost (€/t)	653	Ship and bunker (2019), average Nov 2014 – Nov 2019
Lubricant cost (€/t)	1600	Industry sources
Single pressure WHR capital cost for reference engine MCR power (€/kW)	98.7	DSME (2008), values adapted to 2015
Single pressure WHR reference engine MCR power (kW)	8775	DSME (2008)
Dual pressure WHR capital cost for reference engine MCR power (€/kW)	95.96	DSME (2008), values adapted to 2015
Dual pressure WHR reference engine MCR power (kW)	29260	DSME (2008)
Scale factor for single pressure WHR	0.75	Assumption
Scale factor for dual pressure WHR	0.75	Assumption
Steam turbo-generator capital cost factor for the reference nominal electric power (€/kW)	1067	DOE (2016)
Steam turbo-generator reference nominal electric power (kW)	500	DOE (2016)
Steam turbo-generator scale factor	0.72	Calculated from DOE (2016)
Maintenance cost for WHR (% of investment cost /year)	2%	Industry sources

466 **5.5 Parameters selection for the sensitivity analysis**

467 A sensitivity analysis determines how the different input parameters affect the model results. In this study,
468 the input parameters identified as candidates for performing a sensitivity study were: the fuels prices, the engine
469 operating profile, the WHR system capital cost, the discount rate, the sizing of the WHR system components, and
470 the steam drum(s) pressures. The need for sensitivity analysis for each of these parameters is assessed based on
471 their variability and the expected influence on the results, as discussed below.

472 The influence of the engine operating profiles was highlighted in Section 5.3. It is expected that the
473 investigated ships operating profile will not vary considerably in the future. The WHR system capital cost can
474 have considerable influence on the results; however, since these systems are well established commercial
475 technologies, the capital cost is highly unlikely to vary significantly. The discount rate influence on the results is
476 estimated to be moderate; moreover, the discount rate values have not varied much in the past for the shipping
477 industry as reported in Tsereklas-Zafeirakis et al. (2016). The steam pressure affects the steam power plant

efficiency; however, the expected variability of the steam pressure is small when taking into account the limitations imposed due to the specific engine exhaust gas temperature ranges and the WHR systems operational requirements (SNAME, 1990) (MAN, 2014). The only parameters that are expected to considerably influence the results include the WHR system components size and the fuels prices. These parameters are discussed in the subsequent sections.

5.5.1 WHR systems turbo-generator size

Considering the engine operating profiles presented in Fig. 5, it can be inferred that the Handymax tanker engine spends considerable time operating in low loads. As deduced from Fig. 4, the exhaust gas thermal power considerably reduces at low engine loads. Thus, using a turbo-generator sized for the engine full load conditions will lead to an inefficient WHR system at part loads, reducing its potential for generating electric power. This may render the system unfeasible also considering the cost of installation and the required components volume. To avoid WHR system inefficient operation, the engine manufacturers recommend the WHR system deactivation (using bypass valves) when the engine operates at loads below 50% of MCR (MAN, 2012). In these cases, the ship auxiliary boiler is used to generate the required saturated steam.

When sizing the WHR systems components at part load conditions, an upper threshold in the generated electric power (turbo-generator rated power) is expected at high engine loads, however a higher electric power can be obtained at lower engine loads, thus extending the WHR system operating range. In this case, bypassing (by appropriate valves control) a percentage of the exhaust gas around the WHR system boiler is required at high engine loads for operating the turbo-generator at its rated power and avoiding its overloading.

To investigate this issue, the present study considers the following two cases for the rated (nominal) sizing of the WHR1 and WHR2 systems turbo-generator: (i) nominal power matches the vessel main engine full load conditions; (ii) nominal power matches the ship main engine operation at part loads. For the latter case, it is assumed that an exhaust gas bypass valve is used, thus limiting the generated electrical power when the ship main engine operates at the high load region. The considered nominal power values of the two WHR steam systems for the investigated tanker vessels are reported in Table 5. These values were derived following a parametric study optimisation with an objective to maximise the annual fuel savings. This optimisation study along with its results are not presented herein.

Table 5. Turbo-generator nominal power for the investigated ships.

	Handymax tanker		Suezmax tanker		VLCC	
	Full load design	Part load design	Full load design	Part load design	Full load design	Part load design

Turbo-generator nominal power for single pressure WHR system (kW)	250	100	640	400	800	500
Turbo-generator nominal power for dual pressure WHR system (kW)	250	100	800	500	1000	640

5.5.2 Fuels price

Due to the fact that the fuels prices have been fluctuating significantly in the past and considering that they are one of the major revenue factors influencing the feasibility of the investigated WHR options, a sensitivity analysis was performed to quantify the varying fuels prices impact. For this purpose, a range of 60% above and below the baseline values, that lie within the extreme values that have been observed for fuel prices for the last decade (between 2009 and 2019) was used as shown in Table 6.

Table 6. Fuel prices used for sensitivity analysis.

Fuel Prices	**HFO (€/t)**	**MGO (€/t)**
High price (+60%)	605.0	991.5
Baseline	378.1	619.7
Low Price (-60%)	151.3	247.9

6 Results and discussion

6.1 WHR systems performance parameters

The derived performance parameters of the investigated WHR systems and turbo-generator sizes (at full load and part load conditions) for the Suezmax tanker, including the generated electric power and respective efficiency increase, the steam cycle efficiency as well as the boiler HP evaporator pinch point temperature difference, are presented in Fig. 6. It can be deduced that the WHR2 system performance, in terms of the generated electric power and the steam cycle efficiency, surpasses by 25% on average the one of the WHR1 system in the whole engine operating envelope apart from the 25% load, where both the WHR systems generate almost the same electric power (around 30 kW). Considering the WHR systems with the sized turbo-generator at engine part load conditions, the generated electric power reaches the rated electric power above 85% load, as the exhaust gas bypasses the boiler.

In the engine load range 40% to 75%, the WHR1 system sized at engine part load conditions (WHR1-part load) generates more power (an increase of 13-18% is obtained) in comparison to the case when the system turbo-generator is sized for the engine full load (WHR1-full load). Similarly, the WHR2 system sized at part load conditions (WHR2-part load) generates 8-12% additional electric power in comparison with the case when the

system turbo-generator is sized at full load (WHR2-full load). When the ship main engine operates at 25% load, the WHR systems electric power output is comparable due to the very low available exhaust gas energy. Based on these results, it can be assumed that the point for cutting off the WHR systems operation with their turbo-generators sized for the engine part load conditions can be extended to down to 40% engine load (instead of the 50% engine load, which was assumed in the case where the WHR systems are sized at the engine full load conditions).

Additionally, it is noted that the overall steam cycle efficiency was relatively low, around 10%, with its maximum being around 15%, which is aligned with previous studies results (Uusitalo et al., 2019). The respective efficiency increase due to the net electric power generation (after subtracting the electric power required for operating the WHR system pumps) is in the range 0.5−2%. However, it must be highlighted that this corresponds to the power plant efficiency increase without burning additional fuel. Hence, the WHR systems installation positively impacts both the ship power system and the environment. The temperature difference at the high pressure pinch point (Fig. 6) was in the range 14-20°C, which is acceptable for these systems design.

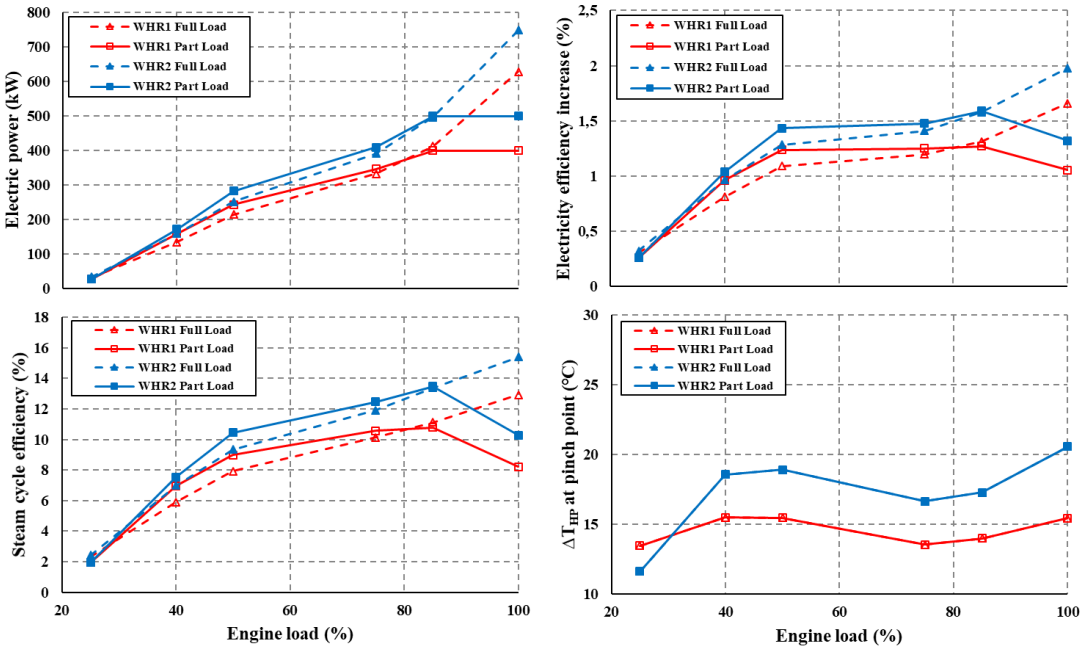

Figure 6. WHR systems calculated parameters for the Suezmax tanker propulsion plant.

6.2 Fuels and lubricating oil savings

The energy saving potential of both WHR systems are first investigated comparing with the performance of the baseline power plant considering the three vessels and the two cases of the WHR systems turbo-generator sizing. For the three investigated vessels, the simulation results as well as the calculated fuel and lubricating oil (LO) savings comparing with the baseline case respective results are presented in Table 7.

546 The derived results presented in Table 7 demonstrate that compared to the baseline plant, savings in the range
547 1%−8.1% for the fuels (HFO and MGO) consumption, and 2%−11.9% for the lubricating oil consumption can be
548 obtained when using the WHR systems. As the same engines operating profiles were assumed for sailing inside
549 and outside ECAs, the same percentage savings were calculated for the HFO and MGO. For all the investigated
550 ships, the WHR2-part load system exhibited the greatest savings in both the fuel and the lubrication oil
551 consumptions.

552 However, these savings vary based on the ship size. For the smallest size vessel (Handymax tanker), the
553 WHR2 system exhibited around 0.25% lower fuel consumption (4.5 t of HFO and 4.3 t of MGO annually)
554 compared to the WHR1 system. For the Suezmax vessel and the VLCC, this difference (fuel savings between the
555 WHR1 and WHR2 systems) is even smaller and equals to around 0.1%. For the VLCC, the maximum achieved
556 fuel savings are about 1136 t/year (out of which 19% was MGO) (for the WHR2-part load system). For the
557 Handymax tanker, fuel savings about 176 t/year (out of which 49% was MGO) can be obtained (also for the
558 WHR2-part load sytem). As the Handymax tankers operate more extensively in ECAs, which requires MGO to
559 comply with the existing regulations, the WHR systems installed on-board these vessels are expected to have
560 higher relative impact on the MGO consumption compared to the HFO consumption.

Table 7. Simulation results for the investigated vessels for the cases of turbo-generator sized at main engine full load and part load conditions.

	Handymax tanker			Suezmax tanker			VLCC		
	Baseline	WHR1	WHR2	Baseline	WHR1	WHR2	Baseline	WHR1	WHR2
Turbo-generator sized at the ship main engine full load conditions									
Fuel			t/year						
FC AE HFO	160.0	157.5	154.4	571.3	412.6	385.5	877.5	656.4	634.2
FC AE MGO	151.8	149.4	146.4	135.5	97.8	91.4	208.1	155.6	151.2
FC boiler HFO	64.9	54.4	54.4	442.5	210.0	210.0	573.8	272.5	272.5
FC boiler MGO	61.6	51.6	51.6	104.9	49.8	49.8	136.1	64.6	64.6
FC HFO Total	1287.3	1274.2	1271.1	8557.1	8165.8	8138.7	13913.9	13391.5	13369.3
FC MGO Total	1221.0	1208.6	1205.6	2029.1	1936.3	1929.9	3299.2	3175.4	3170.9
HFO saving	-	13.1 (1.0%)	16.2 (1.3%)	-	391.3 (4.6%)	418.4 (4.9%)	-	522.4 (3.8%)	544.6 (3.9%)
MGO saving	-	12.4 (1.0%)	15.4 (1.3%)	-	92.8 (4.6%)	99.2 (4.9%)	-	123.9 (3.8%)	128.4 (3.9%)
Lubricating Oil (LO)	t/year								
LO consumption	9.4	9.3	9.3	43.1	41.7	41.7	70.2	68.1	68.1
LO saving	-	0.2 (2.0%)	0.2 (2.0%)	-	1.4 (3.2%)	1.4 (3.2%)	-	2.1 (3.0%)	2.1 (3.0%)
CAPEX (€)		797,567	1,047,651		1,532,753	2,013,359		2,265,541	2,975,918
Yearly Cash Flow (€/year)		12,949	15,927		202,721	219,588		274,528	288,846
Turbo-generator sized at the ship main engine part load conditions									
Fuel			t/year						
FC AE HFO	160.0	139.2	134.7	571.3	355.6	322.5	877.5	545.4	512.8
FC AE MGO	151.8	132.1	127.8	135.5	84.3	76.5	208.1	129.3	122.2
FC boiler HFO	64.9	0	0	442.5	0	0	573.8	0	0
FC boiler MGO	61.6	0	0	104.9	0	0	136.1	0	0
FC HFO Total	1287.3	1201.6	1197.1	8557.1	7898.9	7865.8	13913.9	13007.9	12975.3
FC MGO Total	1221.0	1139.7	1135.4	2029.1	1873.0	1865.1	3299.2	3084.4	3077.3
HFO saving	-	85.7 (6.7%)	90.3 (7.0%)	-	658.2 (7.7%)	691.3 (8.1%)	-	905.9 (6.5%)	938.5 (6.7%)
MGO saving	-	81.3 (6.7%)	85.6 (7.0%)	-	156.1 (7.7%)	163.9 (8.1%)	-	214.8 (6.5%)	221.9 (6.7%)
Lubricating oil (LO)	t/year								
LO consumption	9.4	8.3	8.3	43.1	40.5	40.5	70.2	66.2	66.2
LO saving	-	1.1 (11.9%)	1.1 (11.9%)	-	2.6 (6.0%)	2.6 (6.0%)	-	4.0 (5.7%)	4.0 (5.7%)
CAPEX (€)		625,588	875,671		1,332,701	1,778,691		2,030,872	2,712,428
Yearly Cash Flow (€/year)		84,590	88,974		350,571	366,576		482,271	495,491

563 **6.3 Economic analysis results**

564 The Net Present Value (NPV) and Profitability Index (PI) results for the two WHR systems
565 investments sized at for both engine full and part load conditions for the three different ships are
566 compared in Fig. 7 and Fig. 8, respectively. It must be noted that the calculated cash flows do not take
567 into account the ship earnings and the transported cargo.

568 In terms of the investigated WHR systems, the single pressure WHR solutions appear to be more
569 profitable than the dual pressure WHR systems under the cost assumptions made for all ship sizes. The
570 dual pressure WHR system is less attractive in terms of investment yield due to the higher investment
571 cost not being accompanied by equal magnitude of cost savings.

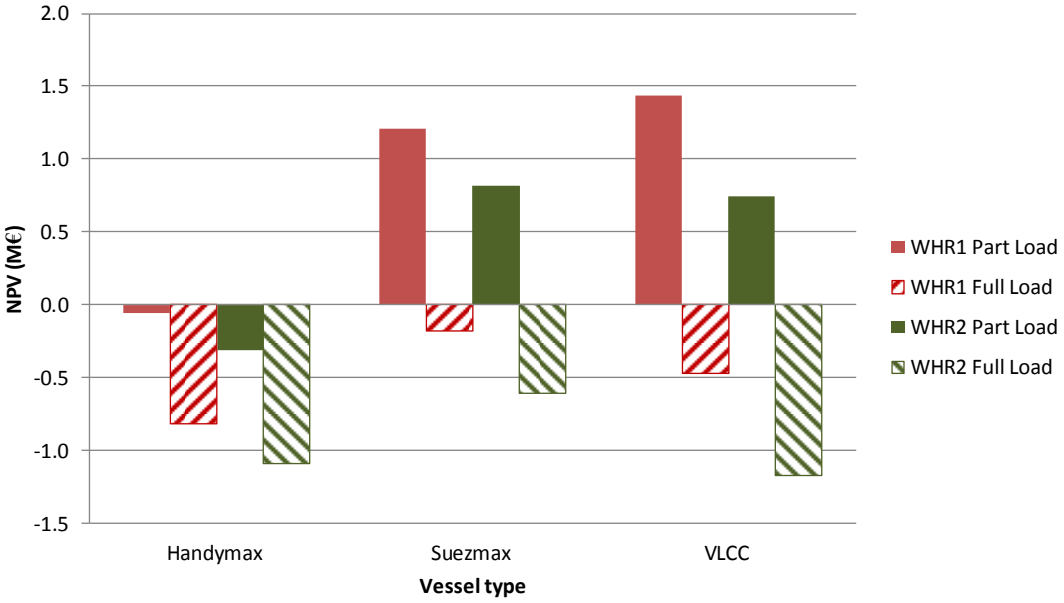

572

573 **Figure 7.** Net Present Value of the investigated WHR systems.

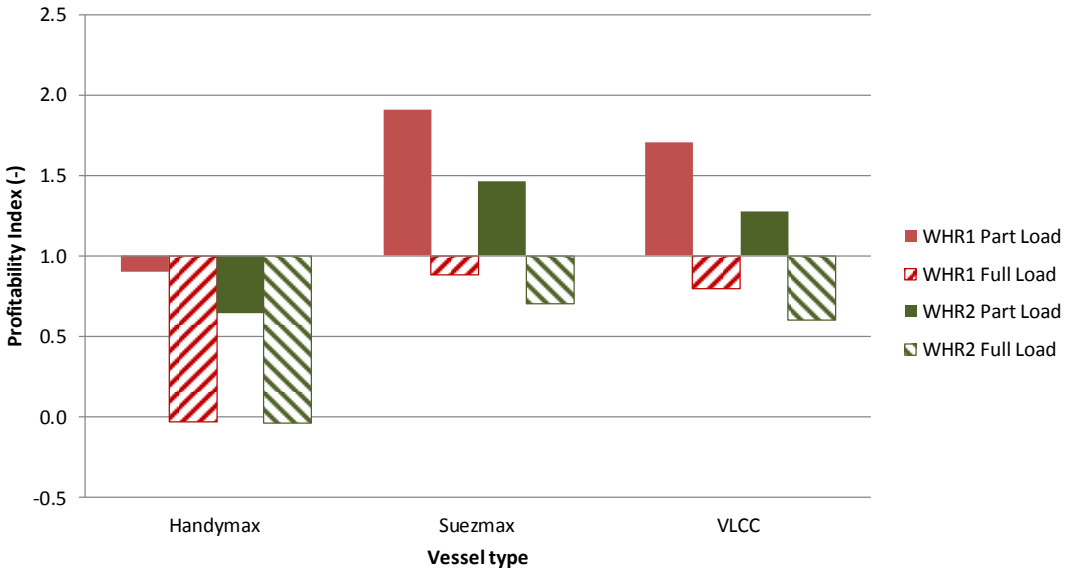

574

575 **Figure 8.** Profitability Index of the investigated WHR systems.

576

577 Furthermore, the WHR systems sized at engine part load conditions always lead to a better
578 investment yield for all the ship sizes, and are profitable options for both single and dual pressure WHR
579 systems for larger ship sizes (Suezmax and VLCC). This result confirms the suitability of part-load
580 design compared to the traditional full-load design given the currently established practice of engine low
581 loads operation (or slow steaming), as it can considerably improve the performance of the WHR systems,
582 and hence their financial attractiveness.

583 In terms of the ship size, it can be concluded that both the Suezmax tanker and the VLCC are good
584 candidates for installing WHR systems, in particular of the single pressure type, provided that the part-
585 load design is adopted. Although the dual pressure WHR system can still be profitable when its design
586 is sized at engine part load conditions, the investment yield is lower than the single pressure system and
587 therefore, it could more easily turn into negative, should the investment or operating conditions change.
588 For the Handymax tanker, the WHR systems always exhibited a negative investment yield; this is
589 attributed to the specific operating profile spanning in the low to medium engine loads as well as the fact
590 that the larger ships benefit from the economies of scale that reduce the cost per unit of WHR system
591 installed capacity. It is interesting to note though that the Suezmax tanker exhibited a slightly higher
592 return on investment than the VLCC, despite the fact that the theoretical economies of scale for the capital
593 cost are in favour of the larger size VLCC.

.

6.4 Environmental parameters results

The fuel savings of the investigated WHR systems compared to the baseline case are presented in Fig. 9. The fuel savings for the WHR1 systems are always lower than the respective ones of the WHR2 systems for all ship sizes; they are much higher for the WHR system designed at engine part load conditions. It is also inferred that the WHR design at engine full load leads to significantly less fuel savings in all cases, due to the impact of low engine load operation and the subsequent reduction in the effective WHR systems operational time. Fuel savings for the WHR systems sized at engine full load conditions range from the minimum of 1% for the Handymax tanker to the maximum of 4.8% for the Suezmax tanker. One of the main underlying reasons for the Suezmax tanker higher return on investment than the VLCC in any WHR system is the higher annual fuel savings (as shown in Fig. 9). The significant difference in fuel savings between the WHR systems design at engine part-load and full-load conditions is the primary reason behind the significantly better return on investment of the former, irrespective of the ship size and technology adopted.

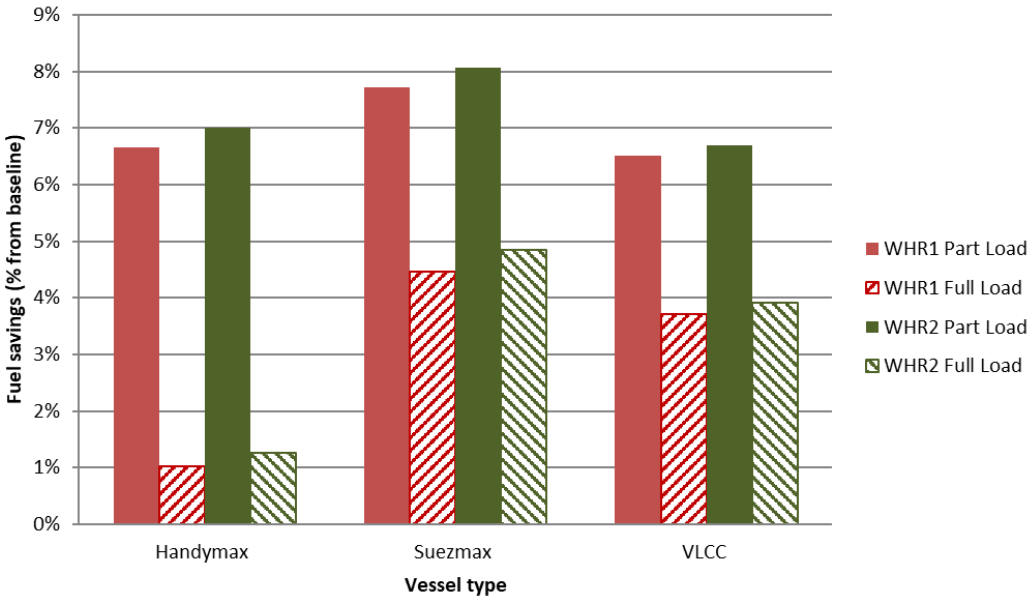

Figure 9. Fuel savings of the investigated WHR systems compared to baseline configuration.

The fuel savings of the different system configurations against the baseline are also converted into CO_2 equivalent emission reductions (Fig. 10a). For the purposes of this study, the CO_2 emissions were not converted into an economic benefit for the system. In the future, where a CO_2 tax may be introduced, installing a WHR system would lead to further savings through reducing the CO_2 equivalent emissions.

It is deduced from Fig. 10 that the higher CO_2 equivalent emission reductions occur for the system

615 configurations that already have the best financial yield, i.e. the Suezmax tanker and the VLCC for WHR
616 systems design at the engine part load conditions, with very similar CO_2 reduction levels for both the
617 single and dual pressure WHR systems. This means that these configurations would be even more
618 attractive should these additional savings be monetised and included in the investment analysis. The
619 difference in the CO_2 reductions achieved through design at engine full or part-load can be substantial in
620 small size ships; for the Handymax vessel, the single and dual pressure WHR systems exhibited
621 significantly higher CO_2 emission reductions when designed at engine part-load conditions (compared
622 to designs at the engine full-load).

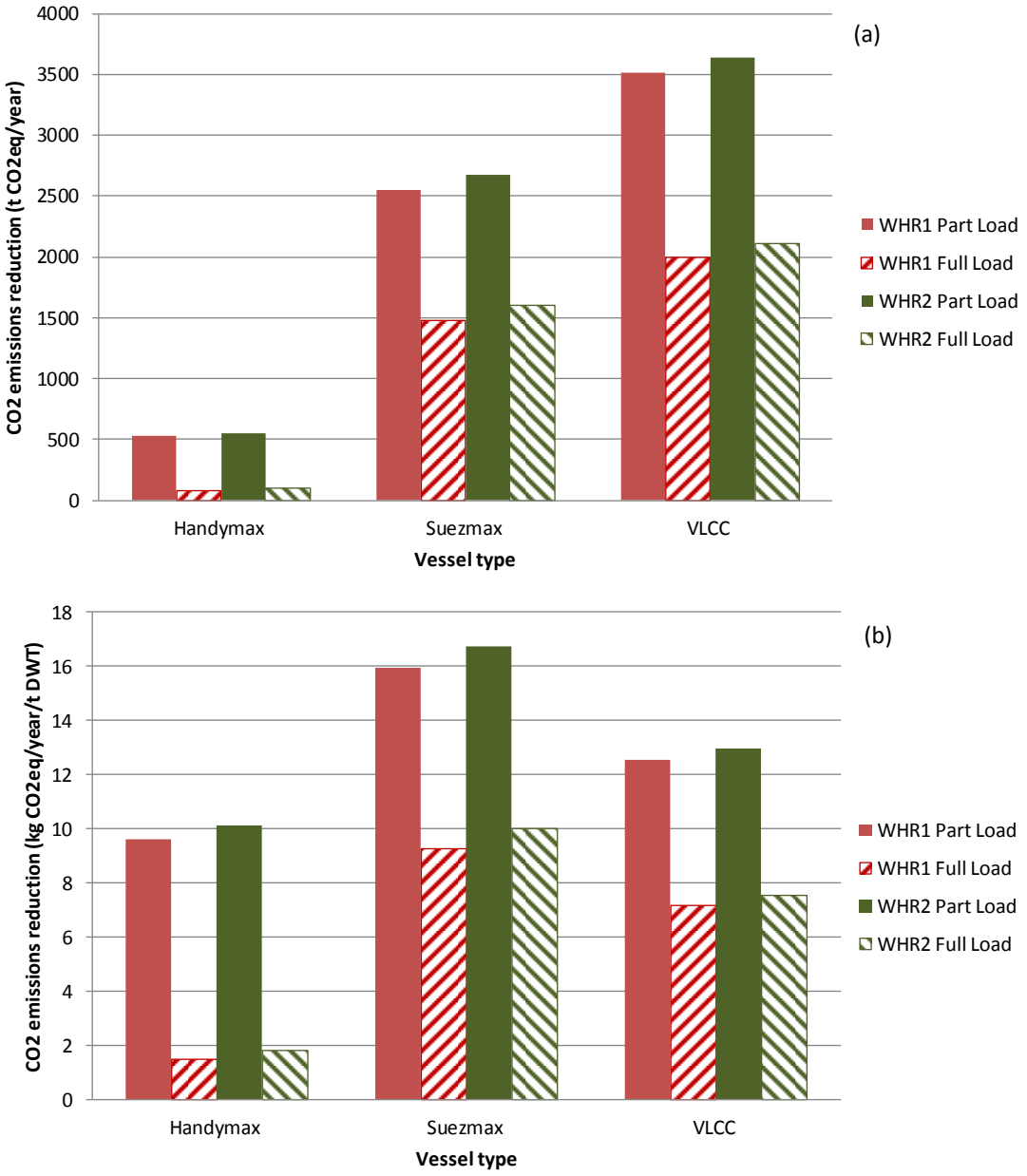

623

.

Figure 10. Annual CO_2 equivalent emission reductions for the WHR systems compared to the baseline system; (a) in kg CO_2/year; (b) normalised by the ship deadweight (in kg CO_2/year/t DWT).

For bigger ships, this difference is still considerable, although not as profound; with the Suezmax tanker exhibiting 68% (WHR1) and 57% (WHR2) increases in CO_2 emission reductions under the engine part-load conditions designs compared to the full-load. The corresponding figures for the VLCC are 75% and 69%, respectively. When considering the ships typical lifetime (assumed 25 years in this study), the CO_2 equivalent emission reductions for the VLCC could add up to 88950 tons with the WHR2-part load system, or 87750 tons for the WHR1 system-part load system. Considering the normalised annual CO_2 emission reductions by the ships deadweight (Fig. 7b), the WHR systems designed at the engine part-load conditions for the Suezmax Tanker exhibit the highest performance of this metric, followed by the respective systems for the VLCC and the Handymax size tanker. A similar trend, however with considerably reduced performance on this metric, is observed in the case of the WHR systems designed at the engine full load conditions. These results indicate that the larger ships (Suezmax tankers and VLCC) carbon footprint will be considerable improved by installing WHR systems; however the appropriate sizing needs to be selected to match the vessel operating profile in order achieve the maximum benefit.

6.5 Fuels prices sensitivity analysis

The results of the sensitivity analysis are presented in Fig. 11(a and b). It can be inferred that the fuel prices can have a major impact on the profitability of the WHR systems. For example, no type of WHR technology is profitable irrespectively of the vessel size under the low fuel price scenario. In this case, the fuel savings (presenting the revenues for the investment) are simply not enough to justify the investment. On the other hand, the higher fuel prices render all the WHR options profitable for the Suezmax tanker and the VLCC. For the Handymax tanker, most technologies are still not profitable, except for the WHR1-part load system, which is marginally profitable. Thus, large vessels seem to benefit substantially in terms of the WHR technologies profitability from increased fuel prices.

It can also be inferred that the relative performance of the various technologies remains unchanged irrespectively of the fuel price levels; for any vessel size, the WHR1-part load system is the most promising solution, followed by the WHR1-part load system. The WHR systems designed at engine full load always perform worse in investment yield terms than the systems designed at engine part load using the same technology.

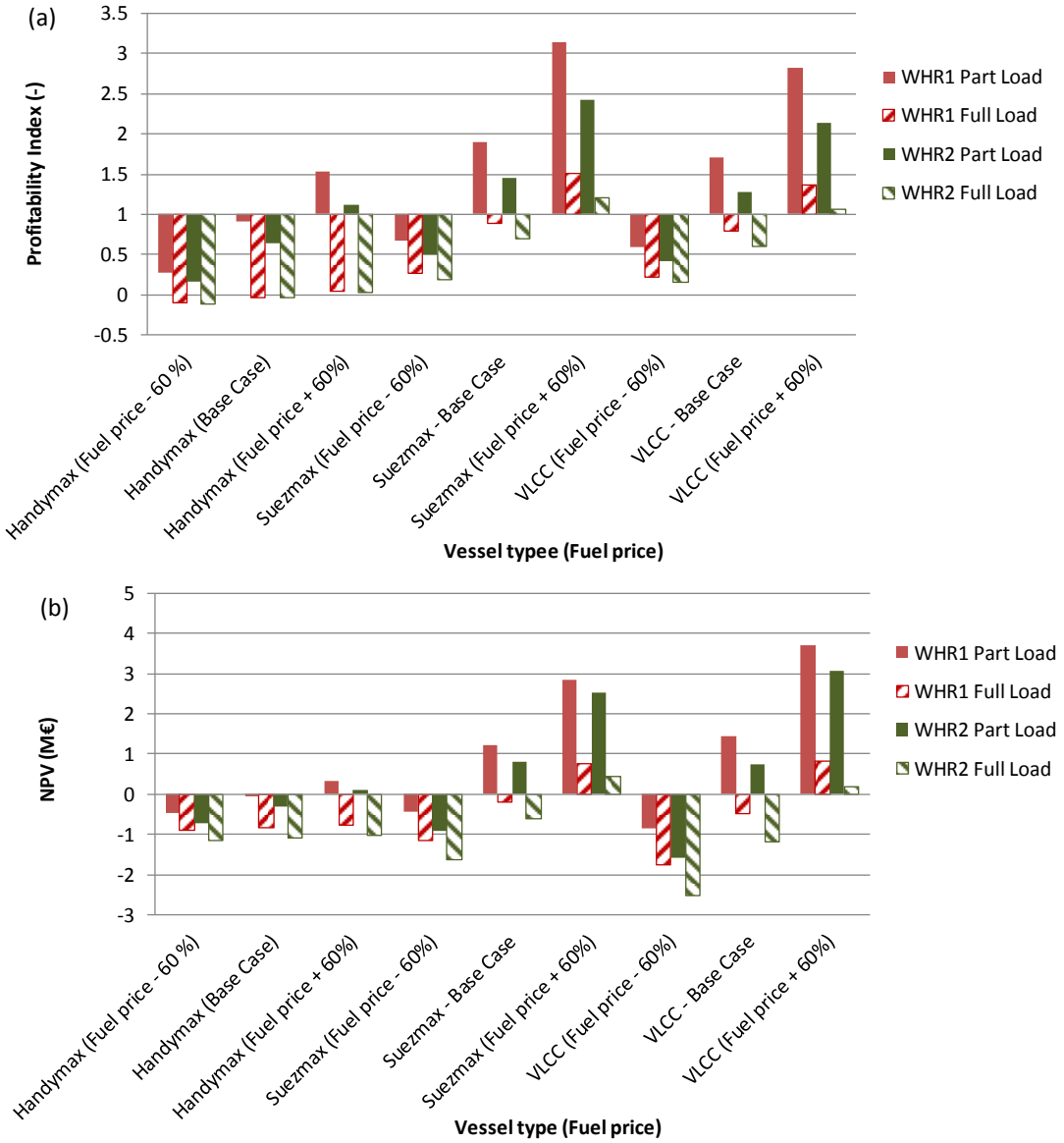

Figure 11. Fuel price sensitivity analysis results: (a) impact on Profitability Index; (b) impact on Net Present Value.

To provide a better understanding of the viability of the investigated WHR options, the marginal values of the HFO price that render each scenario profitable were identified in Fig. 12. It was assumed that the MGO price remains linked to that of HFO by a factor of 1.64, which stems from the fuels price values adopted. Since the fuel prices were extremely volatile in the past, indicating significant uncertainty for the future, decision makers (ship designers/operators) can use this chart to make informed decisions on the WHR technology selection based on their expectations for the average future fuel prices. The main findings from Fig. 12 are aligned with those from Fig. 11, as most of the WHR options for the Handymax

vessel require unrealistically high fuel prices for rendering them a worthwhile investment, whereas for the Suezmax tanker and the VLCC, most options are within the historical fuel price ranges. Particularly the option of WHR1-part load system would require fuel prices above 212 €/t and 235 €/t for positive return on investment for the Suezmax and VLCC respectively, which is significantly lower than the fuel prices observed in 2018.

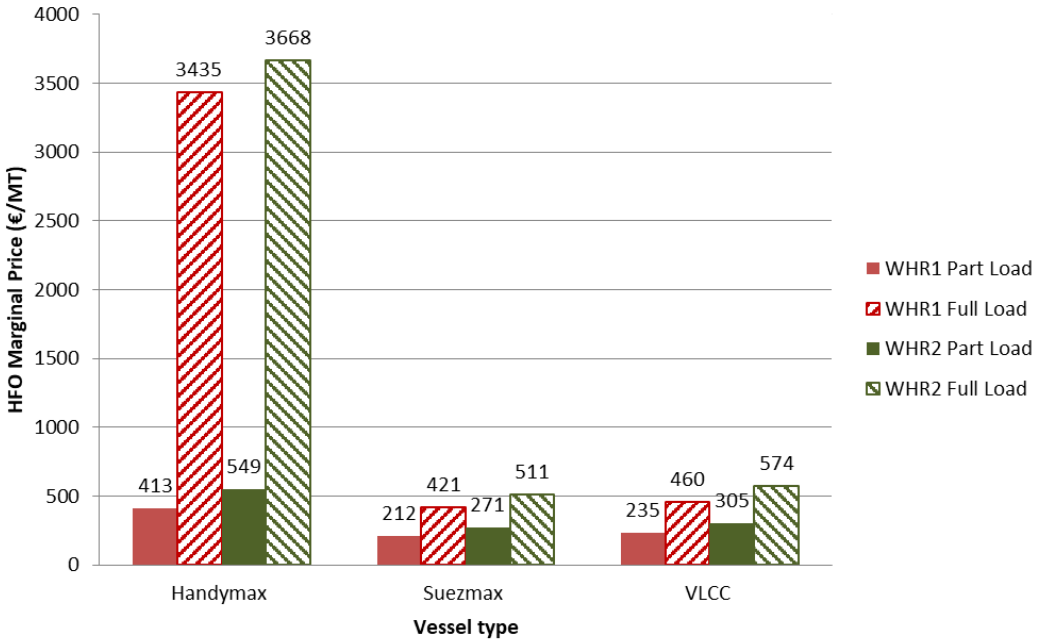

Figure 12. Marginal HFO prices to make each WHR technology profitable.

6.6 Implications to theory and ship systems sustainability

This study presented a methodology to analyse the techno-economic and environmental impacts of various WHR systems designs on actual ships operations. Therefore, this study provides the required numerical tools and framework for obtaining a better understanding and more thorough insights of the underlying parameters that influence the technical, economic and environmental performance of the WHR systems operation for ocean-going vessels. The proposed methodology can be customised and applied for other ships types or extended to include other energy efficiency improvement technologies.

This study supports the sustainability enhancement of the ships systems by identifying feasible commercially available WHR steam systems, leading to fuel savings and carbon emissions reduction whilst simultaneously increasing the power plant economic performance. Considering the immense pressure in the shipping industry for reducing the carbon emissions, this study supports the decision-making process as the anticipated impacts for the candidate energy efficiency systems can be evaluated

in the ship design phase. The shipping industry conservatism is widely acknowledged, with the majority of the ship owner reacting retrospectively to comply with imposed regulations. This is partially attributed to the lack of persuasive evidence for the impact of the proposed technologies. Considering the recent investments (amounting to $1-3 million per system per ship) to install ballast water treatment systems and exhaust gas scrubbers for complying with the existing regulations, the installation of optimally designed WHR steam systems will be a solution towards improving the sustainability of large ocean going ships. It was demonstrated from the results of this study that the WHR steam systems sized to match the ship engine part load operation are readily available solutions providing techno-economic-environmental benefits. In this respect, this study provides the scientific ground for understanding the benefits of these WHR systems, so that the ship owners/operators are convinced to install them on both existing and new-built ships. Although the carbon emissions were not monetized, it is expected that a potential introduction of a carbon tax in the shipping sector will create additional pressure for installing practical and feasible carbon reduction technologies on-board ships. In this case, the present study methodology can be employed for quantifying profitability and carbon reduction benefits and provide the required data for decision making in the shipping industry stakeholders.

7. Conclusions

This study employed state-of-the-art thermodynamic modelling, economic and environmental analysis tools to systematically assess the impacts of the WHR steam systems alternative designs. The proposed methodology took into account the actual expected annual voyages details, the engines operating profiles as well as the investigated systems actual operation. The influence of the WHR system type, their turbo-generator sizing, the fuel prices and the ship size on the techno-economic and environmental performance was quantified.

It is concluded that the obtained efficiency increase (0.8−1.6% for the single pressure system; 1−2% for dual pressure system) does not seem very attractive for supporting these systems on-board installation. This is aligned with the current practice and perception of the ship owners/operators. However, when considering the actual ships operating profiles and the calculated fuel savings, it was found that some WHR steam systems designs (in particular the designs at the engine part-load) can become attractive solutions, as they provided fuel savings in the range 6.5−8.1% (outperforming the WHR systems sized at engine full load conditions). In addition, non-attractive designs for specific ships were identified (for

example, for the Handymax tanker).

Focusing on the investigated systems environmental performance, although it was found that the annual CO_2 emissions reductions in absolute terms are proportional to the ship size, the comparison in relative terms (CO_2 emissions reductions per ship deadweight) promoted the middle size ships , followed by the largest ships size, whereas the smallest ships ranked last. The dual pressure WHR system with its components sized at the engine part-load conditions was found to exhibit the highest impact on both the fuel savings and the CO_2 emissions reduction for all the investigated ships, however it only slightly outperforms the single pressure system sized at part-load conditions.

This trend reverses when considering the economic parameters assessment, as the single pressure systems sized at engine part-load were found to be more profitable compared to the dual pressure systems, due to the higher investment cost of the latter. In addition, the installation of all the investigated systems was not profitable for the smallest size ship, which indicates that other technologies (or combinations of systems) need to be investigated for enhancing these ships sustainability. Moreover, the systems sized at engine full load conditions were found to be non-profitable in all ships. This implies that designs optimised for one operating point are not feasible and the engine operating profile is a critical parameter that needs to be taken into account in the ship design phase for ensuring the system sustainability.

As expected, the fuel prices greatly influence the WHR systems profitability, with low fuel prices leading to non-profitable systems for all the investigated vessels types. Considering the estimated HFO marginal prices, the ranking of the ship attractiveness for WHR systems installation was the same as reported for the environmental parameters assessment (middle size, largest size, smallest size). For the Suezmax tanker and the VLCC, the investigated systems can become profitable within HFO price ranges that have been historically observed; the single pressure WHR systems sized at engine part-load exhibited the lowest marginal prices (€212 for the Suezmax tanker, €235 for the VLCC). For the Handymax tanker, only the single pressure WHR system sized at engine part-load was found to be marginally profitable.

Based on the preceding points as also considering the complexity of the dual pressure WHR steam systems, it can be concluded that the installation of single pressure WHR systems optimally designed to match the ship actual operating profile is recommended for the ships in the middle and largest sizes, whereas other solutions for decarbonisation need to be investigated for the smallest size vessels. However, it must be noted that this study did not consider the effects of the exhaust system back pressure variability

due to the boiler design and fouling on the overall performance as well as the influence of the carbon tax on the systems profitability. These topics along with the optimisation of the WHR systems design considering actual operating conditions and implementation of WHR systems in other ship types can be investigated in forthcoming studies. Future research is expected to focus on holistic approaches for investigating solutions and technologies to address the shipping sector unprecedented challenges and the quest for ensuring its sustainability.

Acknowledgements

The authors affiliated with the Maritime Safety Research Centre greatly acknowledge the financial support by the MSRC sponsors DNV GL and RCCL. The opinions expressed herein are those of the authors and should not be construed to reflect the views of DNV GL AS, RCCL. The research work performed by Dr. Guan was supported by National Natural Science Foundation of China (51579200), Natural Science Foundation of Hubei Province of China (2018CFB364), key laboratory of marine power engineering and technology authorized by MOT (KLMPET2018-03) and the fundamental research funds for the general universities (2019III046GX).

References

Ahmed, A., Khodary Esmaeil, K., Irfan, M. A., Al-Mufadi, F. A., 2018. Design methodology of heat recovery steam generator in electric utility for waste heat recovery. International Journal of Low-Carbon Technologies 13(4), 369–379.

Altosole, M., Laviola, M., Trucco, A., Sabattini, A., 2014. Waste Heat Recovery systems from marine diesel engines: Comparison between new design and retrofitting solutions. Maritime technology and engineering, 735-742.

Ancic, I., Vladimir, N., Runko Luttenberger, L., 2018. Energy efficiency of ro-ro passenger ships with integrated power systems. Ocean Engineering 166, 350-357.

Balcombe, P., Brierley, J., Lewis, C., Skatvedt, L., Speirs, J., Hawkes, A., Staffell, I., 2019. How to decarbonise international shipping: Options for fuels, technologies and policies. Energy Conversion and Management 182, 72-88.

Baldi, F., Larsen, U., Gabrielii, C., 2015. Comparison of different procedures for the optimisation of a combined Diesel engine and organic Rankine cycle system based on ship operational profile. Ocean

Engineering 110, 85-93.

Banks, C., Turan, O., Incecik, A., Theotokatos, G., Izkan, S., Shewell, C., Tian, X., 2013. Understanding ship operating profiles with an aim to improve energy efficient ship operations. Proceedings of the Low Carbon Shipping Conference, London, UK, 9–10 September 2013.

Basurko, O.C, Mesbahi, E. Methodology for the sustainability assessment of marine technologies. Journal of Cleaner Production, 68(2014), 155-164. DOI:10.1016/j.jclepro.2012.01.022.

Benvenuto, G., Trucco, A., Campora, U., 2014. Optimization of waste heat recovery from the exhaust gas of marine diesel engines. Proc Inst Mech Eng, Part M: J Eng Marit Environ 230 (1), 83-94.

Bolbot, V., Trivyza, N.L., Theotokatos, G., Boulougouris, E., Rentizelas, A., Vassalos, D. Cruise ships power plant optimisation and comparative analysis. Energy, 196(2020), 117061. DOI:10.1016/j.energy.2020.117061.

Bouman, E.A., Lindstad, E., Rialland, A. I., Strømman, A.H., 2017. State-of-the-art technologies, measures, and potential for reducing GHG emissions from shipping – A review. Transportation Research Part D: Transport and Environment 52(A), 408-421.

Brynolf, S., Fridell, E., Andersson, K. Environmental assessment of marine fuels: liquefied natural gas, liquefied biogas, methanol and bio-methanol. Journal of Cleaner Production, 74(2014), 86-95. DOI:10.1016/j.jclepro.2014.03.052.

Burel, F., Taccani, R., Zuliani, N., 2013. Improving sustainability of maritime transport through utilization of Liquefied Natural Gas (LNG) for propulsion. Energy 57, 412-420.

Choi, B. C., Kim, Y. M., 2013. Thermodynamic analysis of a dual loop heat recovery system with trilateral cycle applied to exhaust gases of internal combustion engine for propulsion of the 6800 TEU container ship. Energy 58, 404-416.

DSME, 2008. Waste Heat Recovery System for DSME VLCC. Presentation for Greek Ship-owners 5 Nov 2008 Daewoo Shipbuilding & Marine Engineering Co. Ltd.

Dere, C., Deniz, C., 2019. Load optimization of central cooling system pumps of a container ship for the slow steaming conditions to enhance the energy efficiency. Journal of Cleaner Production, 222, 206-217. DOI: 10.1016/j.jclepro.2019.03.030.

Dimopoulos, G., Georgopoulou, C., Kakalis, N., 2011. Modelling and optimization of an integrated marine combined cycle system. In: Proceedings of the 24th International Conference on Energy, Cost,

Optimization, Simulation and Environmental Impact of Energy Systems (ECOS), Novi Sad, Serbia, 1283–1298.

DOE. 2016. Combined Heat and Power Technology Fact Sheet Series. U.S Department of Energy. DOE/EE-1334. July 2016.

Gilbert, P., Walsh, C., Traut, M., Kesieme, U.,Pazouki, K., Murphy, A. Assessment of full life-cycle air emissions of alternative shipping fuels. Journal of Cleaner Production, 172(2018), 855-866. DOI:10.1016/j.jclepro.2017.10.165.

Grimmelius, H., Boonen, E., Nicolai, H., Stapersma, D., 2010. The integration of mean value first principle diesel engine models in dynamic waste heat and cooling load analysis. CIMAC Congress, Bergen, Norway, paper No 280.

Grljusic, M., Medica, V., Racic, N., 2014. Thermodynamic analysis of a ship power plant operating with waste heat recovery through combined heat and power production. Energies 7, 7368-7394.

Guan, C., Theotokatos, G., Chen, H., 2015. Analysis of two stroke marine diesel engine operation including turbocharger cut-out by using a zero-dimensional model. Energies 8, 5738-5764.

Heywood, J. B. 2018. Internal Combustion Engines Fundamentals. McGrow-Hill, ISBN: 9781260116106.

Hountalas, D. T., Katsanos, C., Mavropoulos, G. C., 2012. Efficiency improvement of large scale 2-stroke diesel engines through the recovery of exhaust gas using a Rankine cycle. Procedia-Social Behav Sci 48, 1444-1453.

Iannaccone, T., Landucci, G., Tugnoli, A., Salzano, E., Cozzani, V., 2020. Sustainability of cruise ship fuel systems: Comparison among LNG and diesel technologies, Journal of Cleaner Production (2020), DOI: /10.1016/j.jclepro.2020.121069.

IMO, 2008. Resolution MEPC.176(58): Amendments to the Annex of the Protocol of 1997 to amend the International Convention for the Prevention of Pollution from Ships, 1973, as modified by the Protocol of 1978 relating thereto (Revised MARPOL Annex VI) . London, UK.

IMO, 2014. Resolution MEPC.245(66), Guidelines on the Method of Calculation of the Attained Energy Efficiency Design Index (EEDI) for New Ships. London, UK.

IMO, 2018. Resolution MEPC.304(72), Adoption of the initial IMO strategy on reduction of GHG emissions from ships and existing IMO activity related to reducing GHG emissions in the shipping

sector. London, UK.

Kalikatzarakis, M., Frangopoulos, C. A., 2014. Multi-criteria selection and thermo-economic optimization of organic rankine cycle system for a marine application. Proceedings of the 27th International Conference on Efficiency, Cost, Optimization, Simulation, and Environmental Impact of Energy Systems (ECOS), Turku, Finland.

Larsen, U., Pierobon, L., Haglind, F., Gabrielii, C., 2013. Design and optimisation of organic rankine cycles for waste heat recovery in marine applications using the principles of natural selection. Energy 55, 803-812.

Larsen, U., Sigthorsson, O., Haglind, F., 2014. A comparison of advanced heat recovery power cycles in a combined cycle for large ships. Energy 74, 260-268.

Livanos, G. A., Theotokatos, G., Pagonis, D. N., 2014. Techno-economic investigation of alternative propulsion plants for ferries and RoRo ships. Energy Conversion and Management, 79, 640-651.

Laulajainen R. 2011. Oil product tanker geography with emphasis on the Handysize segment. Fennia International Journal of Geography. 189(1). 1–19.

Ma, Z., Yang, D., Guo, Q., 2012. Conceptual design and performance analysis of an exhaust gas waste heat recovery system for a 10,000 teu container ship. Pol Marit Res 19(2), 31-38.

Makkonen, T., Inkinen, T. Sectoral and technological systems of environmental innovation: The case of marine scrubber systems. Journal of Cleaner Production, 200(2018) 110-121. DOI:10.1016/j.jclepro.2018.07.163.

MAN Diesel & Turbo, 2011. Basic principles of ship propulsion. Publication no. 5510-0004-02, Copenhagen, Denmark.

MAN Diesel & Turbo, 2012. Waste heat recovery system (WHRS) for reduction of fuel consumption, emissions and EEDI. Publication no. 2210-0136-01, Copenhagen, Denmark.

MAN Diesel & Turbo, 2013. Propulsion trends in tankers. Publication no. 5510-0031-01, Copenhagen, Denmark.

MAN Diesel & Turbo, 2014. Thermo efficiency system for reduction of fuel consumption and CO2. Publication no. 5510-0030-03ppr, Oct 2014, Copenhagen, Denmark.

MAN, 2019. CEAS Engine Calculations. https://marine.man-es.com/two-stroke/ceas, accessed 28 Oct 2019.

Pili, R., Romagnoli, A., Spliethoff, H. 2017. Christoph Wieland. Economic Feasibility of Organic Rankine Cycles (ORC) in Different Transportation Sectors. Energy Procedia 105, 1401-1407.

Qiu, Y., Yuan, C., Tang, J., Tang, X., 2019. Techno-economic analysis of PV systems integrated into ship power grid: A case study. Energy Conversion and Management, 198. DOI: 10.1016/j.enconman.2019.111925.

Rentizelas A., Li J., 2016. Techno-economic and carbon emissions analysis of biomass torrefaction downstream in international bioenergy supply chains for co-firing. Energy 114, 129-142.

Schwartz, H., Gustafsson, M., Spohr, J., 2020. Emission abatement in shipping – is it possible to reduce carbon dioxide emissions profitably? Journal of Cleaner Production, 254, DOI: 10.1016/j.jclepro.2020.120069.

Ship and bunker, 2019. Global average bunker prices. https://shipandbunker.com/prices/av/global/av-glb-global-average-bunker-price, accessed 13 November 2019.

SNAME, 1990. Marine diesel power plant practices. T&R bulletin. Jersey City, USA: The society of naval architects and marine engineering. no. 3-49.

Siu Lee Lam, J., Lai, K-h. Developing environmental sustainability by ANP-QFD approach: the case of shipping operations. Journal of Cleaner Production, 105(2015), 275-284. DOI:10.1016/j.jclepro.2014.09.070.

Song, J., Song, Y., Gu, C. W., 2015. Thermodynamic analysis and performance optimization of an Organic Rankine Cycle (ORC) waste heat recovery system for marine diesel engines. Energy 82, 976-985.

Theotokatos, G, Livanos, G. 2013. Techno-economical analysis of single pressure exhaust gas waste heat recovery systems in marine propulsion plants. Proc Inst Mech Eng Part M J Eng Marit Environ 227, 83–97.

Theotokatos, G., Tzelepis, V., 2015. A computational study on the performance and emission parameters mapping of a ship propulsion system. Proc Inst Mech Eng Part M J Eng Marit Environ, 229 (1), 58-76.

Trivyza, N. L., Rentizelas, A., Theotokatos, G., 2018. Environmental and economic sustainability assessment of emerging cruise ship energy system technologies. Proceedings of the 31st International Conference on Efficiency, Cost, Optimization, Simulation and Environmental Impact of Energy

Systems, June 17th to 21st 2018, Guimarães, Portugal.

Tsereklas-Zafeirakis, A., Aravossis, K., Gougoulidis, G., Pavlopoulou, Y. (2016) Journal of Ship Production and Design, 32(2), May 2016, 130–137. DOI:10.5957/JSPD.32.2.150021

Tsitsilonis, K. M., Theotokatos, G., 2018. A novel systematic methodology for ship propulsion engines energy management. Journal of Cleaner Production 204, 212-236.

Tzortzis, G. J., Frangopoulos, C. A., 2018. Dynamic optimization of synthesis, design and operation of marine energy systems. Proceedings of the Institution of Mechanical Engineers, Part M: Journal of Engineering for the Maritime Environment 233 (2), 454-473.

UNCTAD, 2017. Review of Maritime Transport 2017. ISBN: 978-92-1-112922-9.

Uusitalo, A., Nerg, J., Grönman, A., Nikkanen, S., Elg, M., 2019. Numerical analysis on utilizing excess steam for electricity production in cruise ships. Journal of Cleaner Production 209, 424-438.

Vittorini, D., Cipollone, R., Carapellucci, R., 2019. Enhanced performances of ORC-based units for low grade waste heat recovery via evaporator layout optimization. Energy Convers Manage, 197, 1-16.

Wagner W, Kretzschmar H., 2008. International steam tables. Berlin, Heidelberg: Springer-Verlag.

Wu, W. M., Huang, D. S., 2018. Modelling the profitability of container shipping lines: Theory and empirical evidence. Transport Policy 72, 159-170.

Yang, D., Hu, R., Ma, Z., 2013. Part-load analysis of waste heat recovery system for a 10,000 teu container ship. Int J Heat Technol 31(1), 121-128.

Yang, F., Dong, X., Zhang, H., Wang, Z., Yang, K., Zhang, J., Wang, E., Liu, H., Zhao, G., 2014. Performance analysis of waste heat recovery with a dual loop organic Rankine cycle (ORC) system for diesel engine under various operating conditions. Energy Convers Manage 80, 243-255.

Yang, M. H., 2016. Optimizations of the waste heat recovery system for a large marine diesel engine based on transcritical Rankine cycle. Energy 113, 1109-1124.

Yang, M. H., Yeh, R. H., 2014. Analyzing the optimization of an organic Rankine cycle system for recovering waste heat from a large marine engine containing a cooling water system. Energy Convers Manag 88, 999-1010.

Yun, E., Park, H., Yoon, S. Y., Kim, K. C., 2015. Dual parallel organic Rankine cycle (ORC) system for high efficiency waste heat recovery in marine application. Journal of Mechanical Science and Technology 29 (6), 2509-2515.

Zhang, C., Shu, G., Tian, H., Wei, H., Liang, X., 2015. Comparative study of alternative ORC-based combined power systems to exploit high temperature waste heat. Energy Convers Manage, 89, 541-554.

Zhang, X., He, M., Zhang, Y., 2012. A review of research on the Kalina cycle. Renewable and Sustainable Energy Reviews 16, 5309–5318.

Zhang, H., Guan, X., Ding, Y., Liu, C,. 2018. Emergy analysis of Organic Rankine Cycle (ORC) for waste heat power generation, Journal of Cleaner Production, 183 (2018) 1207-1215. DOI: 10.1016/j.jclepro.2018.02.170.

.

Appendix A.

This Appendix describes the dual pressure WHR steam system (WHR2) model referring to the nomenclature provided in the schematic presented in Fig. 2.The equations derived by the application of energy and mass conservation in the WHR2 system components and the boiler sections are provided in Tables A1, A2 and A3. Table A1 includes the energy conservation equations for the boiler and its sections, Table A2 includes the equations derived by applying the mass conservation for the WHR2 system components, whereas Table A3 contains the equations derived by the application of energy conservation in the other components of the investigated system. In specific for deriving eq. (A2) and (A5), it is considered that subcooled water enters each evaporator (having specific enthalpy h_{1sLP} and h_{2sHP}, for the LP and HP evaporators, respectively). This water is first brought to the respective saturation state and subsequently, partially evaporates. Hence, a mixture of saturated water and saturated steam exits the evaporators. This represents the actual operation of the boiler evaporation sections, where saturated water must always flow the evaporator coils in order to prevent overheating.

Table A1. Energy conservation equations for the WHR2 steam system boiler and its sections.

E/G recovered thermal power	$\dot{Q}_b = \eta_b \dot{m}_g c_{p\_g} \left(T_{0g} - T_{5g}\right) = \\ = \dot{Q}_{ev\_LP} + \dot{Q}_{ec\_HP} + \dot{Q}_{sh\_LP} + \dot{Q}_{ev\_HP} + \dot{Q}_{sh\_HP}$	(A1)
LP Evaporator	$\dot{Q}_{ev\_LP} = \eta_b \dot{m}_g c_{p\_g} \left(T_{4g} - T_{5g}\right) = \\ = \dot{m}_{ev\_LP}(h_{w\_LP} - h_{1sLP}) + \dot{m}_{s\_LP}(h_{s\_LP} - h_{w\_LP})$	(A2)
HP Economiser	$\dot{Q}_{ec\_HP} = \eta_b \dot{m}_g c_{p\_g}(T_{3g} - T_{4g}) = \dot{m}_{ec\_HP}(h_{w\_HP} - h_{1sHP})$	(A3)
LP Superheater	$\dot{Q}_{sh\_LP} = \eta_b \dot{m}_g c_{p\_g}(T_{2g} - T_{3g}) = \dot{m}_{sh\_LP}(h_{2sLP} - h_{s\_LP})$	(A4)
HP Evaporator	$\dot{Q}_{ev\_HP} = \eta_b \dot{m}_g c_{p\_g} \left(T_{1g} - T_{2g}\right) = \\ = \dot{m}_{ev\_HP}(h_{w\_HP} - h_{2sHP}) + \dot{m}_{s\_HP}(h_{s\_HP} - h_{w\_HP})$	(A5)
HP Superheater	$\dot{Q}_{sh\_HP} = \eta_b \dot{m}_g c_{p\_g}(T_{0g} - T_{1g}) = \dot{m}_{sh\_HP}(h_{3sHP} - h_{s\_HP})$	(A6)

η_b: boiler efficiency in the order of 98 - 99% ($1-\eta_b$ represents the boiler thermal losses); $\dot{m}_g$: exhaust gas mass flow rate; c_{p_g}: exhaust gas average specific heat at constant pressure; $\dot{m}_{ev\_LP}$: LP evaporator circulating water mass flow rate; $\dot{m}_{s\_LP}$: LP saturated steam mass flow rate; $\dot{m}_{sh\_LP}$: LP superheated steam mass flow rate, h_{w_LP} and h_{s_LP} : specific enthalpy of the saturated water and steam of the LP steam drum; $\dot{m}_{ev\_HP}$, $\dot{m}_{s\_HP}$, $\dot{m}_{ec\_HP}$, $\dot{m}_{sh\_HP}$, h_{w_HP} and h_{s_HP} : respective parameters of the HP steam drum. In specific for eq. (A2), m_{ev_LP} denotes the mass flow rate of the subcooled water that enters the LP evaporator. This flow rate is first heated from h_{1sLP} (specific enthalpy at the LP evaporator inlet) to h_{w_LP} (specific enthalpy of the saturated water at the considered pressure). Only a part of this flow denoted by m_{s_LP} (mass flow rate of the saturated steam in the Low Pressure part) is evaporated (reaching specific

enthalpy h_{s_LP}). Similar considerations apply for deriving eq. (A5) for the HP evaporator.

Table A2. Mass conservation equations for the WHR2 steam system components.

Feed water tank	$\dot{m}_{fw} = \dot{m}_{s\_hs} + \dot{m}_{s\_hfw} + \dot{m}_c$	(A7)
	$\dot{m}_{fw} = \dot{m}_{fw\_LP} + \dot{m}_{fw\_HP}$	(A8)
Condenser	$\dot{m}_c = \dot{m}_{sh\_LP} + \dot{m}_{sh\_HP}$	(A9)
LP drum	$\dot{m}_{fw\_LP} = \dot{m}_{s\_LP} = \dot{m}_{sh\_LP}$	(A10)
HP drum	$\dot{m}_{fw\_HP} = \dot{m}_{s\_HP} = \dot{m}_{sh\_HP} + \dot{m}_{s\_hs} + \dot{m}_{s\_hfw}$	(A11)

$\dot{m}_{fw}$: feed water pump mass flow rate; $\dot{m}_{s\_hs}$: saturated steam mass flow rate required for covering the ship heating services; $\dot{m}_{s\_hfw}$: mass flow rate of the saturated steam required for heating the feed water to the predetermined temperature, $\dot{m}_c$: condenser pump mass flow rate; $\dot{m}_{fw\_LP}$ and $\dot{m}_{fw\_HP}$: mass flow rates of the feed water entering the LP and HP steam drum, respectively; $\dot{m}_{s\_LP}$ and $\dot{m}_{s\_HP}$: mass flow rates of the saturated steam entering the LP and HP steam drum, respectively; $\dot{m}_{sh\_LP}$ and $\dot{m}_{sh\_HP}$: mass flow rates of the superheated steam entering the LP and HP steam drum, respectively.

Table A3. Energy conservation equations for the dual pressure WHR steam system components.

LP Drum	$\dot{m}_{ev\_LP}(h_{w\_LP} - h_{0sLP}) = \dot{m}_{s\_LP}(h_{w\_LP} - h_{3w})$	(A12)
HP Drum	$(\dot{m}_{ec\_HP} + \dot{m}_{ev\_HP})(h_{w\_HP} - h_{0sHP}) = \dot{m}_{s\_HP}(h_{w\_HP} - h_{3w})$	(A13)
Feed water tank	$\dot{m}_{fw}h_{0w} = \dot{m}_c h_{0sCON} + \dot{m}_{s\_hs}h_{0sHS} + \dot{Q}_{hfw}$	(A14)
Heat provided to the feed water by the saturated steam	$\dot{Q}_{hfw} = \dot{m}_{s\_hfw}(h_{s\_HP} - h_{0sHS})$	(A15)
Jacket cooling water	$\dot{m}_{fw}(h_{2w} - h_{1w}) = \eta_{jwc}\dot{m}_{jwc}(h_{jwc\_i} - h_{jwc\_o})$	(A16)
Air cooler	$\dot{m}_{fw}(h_{3w} - h_{2w}) = \eta_{ac}\dot{m}_a c_{p\_a}(T_{ac\_i} - T_{ac\_o})$	(A17)

$\dot{Q}_{hfw}$: thermal power used for heating the feed water tank; $\dot{m}_{jwc}$: cooling water mass flow rate entering the engine jacket water cooler; h_{jwc_i} and h_{jwc_o} : specific enthalpies of the cooling water entering and exiting the engine jacket water cooler; η_{jwc}: jacket water cooler efficiency ($1-\eta_{jwc}$ is the jacket water cooler thermal losses); $\dot{m}_a$: air mass flow rate entering the engine air cooler; c_{p_a} air average specific heat at constant pressure; T_{ac_i} and T_{ac_o} : the temperatures of the air entering and exiting the engine air cooler, respectively; η_{ac}: air cooler efficiency ($1-\eta_{ac}$ is the air cooler thermal losses).

Combining Eq. (A1) to (A17) and after appropriate manipulation, the following equation is derived for calculating the HP superheated steam mass flow rate:

$$\dot{m}_{sh\_HP} = \frac{\dot{Q}_b - \dot{m}_{s\_hs}\left[r_{ec\_HP}(h_{w\_HP}-h_{1sHP}) + r_{ev\_HP}(h_{w\_HP}-h_{2sHP}) + (h_{s\_HP}-h_{w\_HP})\right]}{\left\{\begin{array}{l}(h_{3sHP}-h_{s\_HP}) + r_{sh\_LH}(h_{2sLP}-h_{s\_LP}) + r_{ec\_HP}(h_{w\_HP}-h_{1sHP}) + r_{ev\_HP}(h_{w\_HP}-h_{2sHP}) \\ +(h_{s\_HP}-h_{w\_HP}) + r_{sh\_LH}\left[r_{ev\_LP}(h_{w\_LP}-h_{1sLP}) + (h_{s\_LP}-h_{w\_LP})\right]\end{array}\right\}} \quad \text{(A18)}$$

where r denotes the mass flow ratios according to the following equations:

$$r_{ec\_HP} = \dot{m}_{ec\_HP}/\dot{m}_{fw\_HP}$$

.

$$r_{ev\_HP} = \dot{m}_{ev\_HP}/\dot{m}_{fw\_HP}$$

$$r_{s\square\_LH} = \dot{m}_{s\square\_LP}/\dot{m}_{s\square\_HP}$$

$$r_{ev\_LP} = \dot{m}_{ev\_LP}/\dot{m}_{fw\_LP}$$

The required power for each pump of the system is calculated by using the following equation:

$$P_i = \dot{m}_i(h_{i\_d} - h_{i\_u}) = \dot{m}_i \Delta p_i/(\eta_i \rho_i) \quad \text{(A19)}$$

where $\dot{m}_i$ denotes the pump mass flow rate, h_{i_u} and h_{i_d} are the fluid specific enthalpies upstream and downstream the pump, Δp_i is the pump pressure increase, η_i is the pump efficiency, and ρ_i is the fluid density.

Considering the states (pressure and temperature) of the superheated steam exiting the LP and HP superheaters and taking into account the respective temperature and pressure drops in the pipe connecting the LP and HP superheaters outlets to the steam turbine, the specific enthalpies of the LP and HP superheated steam entering the steam turbine are calculated. The superheated steam is expanded in the steam turbine, thus providing the required mechanical work to drive the electric generator.

The turbo-generator produced electric power is calculated by using the following equation:

$$P_{el} = \begin{bmatrix} \dot{m}_c \left(h_{sh_{LP_i}} - h_{2sLP_{is}}\right) \eta_{tg_{LP}} f_{b_{LP}} f_{T_{LP}} + \\ +\dot{m}_{sh\_HP}(h_{3sHP} - h_{3sHP\_is}) \eta_{tg\_HP} f_{b\_HP} f_{T\_HP} \end{bmatrix} f_L \quad \text{(A20)}$$

where h_{2sLP_is} and h_{3sHP_is} denote the specific enthalpies of the superheated steam exiting the steam turbine LP and HP stages, respectively, that will be obtained for the case of isentropic turbine processes and are calculated from the steam properties by using the respective stage inlet steam specific enthalpy and specific entropy; η_{tg_LP} and η_{tg_HP} denote the efficiencies of the turbo-generator considering the contribution of the LP and the HP stages, respectively, which are calculated using the inlet pressures and the turbo-generator rated power; f_{b_LP} is the back pressure correction factor for the LP stage of the steam turbine (it is considered to be a function of the inlet and outlet pressures); f_{T_LP} is the temperature correction factor for the LP stage of the steam turbine and is function of the inlet pressure and temperature; f_{b_HP} and f_{T_HP} are the respective correction factors for the HP steam turbine stage respectively, (f_{b_HP} is considered to be 1 as the back pressure of the HP stage equals to the LP stage inlet pressure and much higher than the reference value provided by SNAME (1990); and f_L is the correction factor for the steam turbine load and is calculated by using an iterative process as described in the following paragraphs. Data for the estimation of the turbo-generator efficiencies and the correction factors are given by SNAME

.

(1990).

Considering the mixing process of the steam exiting the HP stage and the LP superheated steam, the following equation is derived for the calculation of the specific enthalpy of the superheated steam entering the steam turbine LP stage, $h_{sh\_LP\_i}$ (which is employed in eq. (A20)):

$$h_{sh\_LP\_i} = \left(\dot{m}_{sh\_HP} h_{sh\_HP\_o} + \dot{m}_{sh\_LP} h_{2sLP}\right)/\dot{m}_c \quad \text{(A21)}$$

The specific enthalpy of the superheated steam exiting the steam turbine HP stage $h_{sh\_HP\_o}$ is calculated according to the following equation that is based on the isentropic turbine efficiency definition equation:

$$h_{sh\_HP\_o} = h_{3sHP} - \eta_{st\_HP}\left(h_{3sHP} - h_{3sHP\_is}\right) \quad \text{(A22)}$$

The steam turbine HP stage efficiency, η_{st_HP}, is calculated according to the following equation considering the AC electric generator efficiency, η_{AC_gen}, and assuming that the turbo-generator mechanical efficiency, η_{tg_mech}, is equal to 0.99:

$$\eta_{st\_HP} = \eta_{tg\_HP} f_{b\_HP} f_{T\_HP} f_L / (\eta_{AC\_gen} \eta_{tg\_mech}) \quad \text{(A23)}$$

The electric generator is considered to be of the alternative current (AC) type. The generator efficiency, η_{AC_gen}, is calculated using the generator efficiency at rated load, η_{gen_rated}, and the generator load correction factor, f_{L_gen}, which are related with the turbo-generator rated power, P_{tg_rated}, and load, L_{tg}, respectively. The generator load is calculated as the ratio of its power and the rated power. The iterative procedure used for calculating the turbo-generator produced electric power is illustrated in Fig. A1.

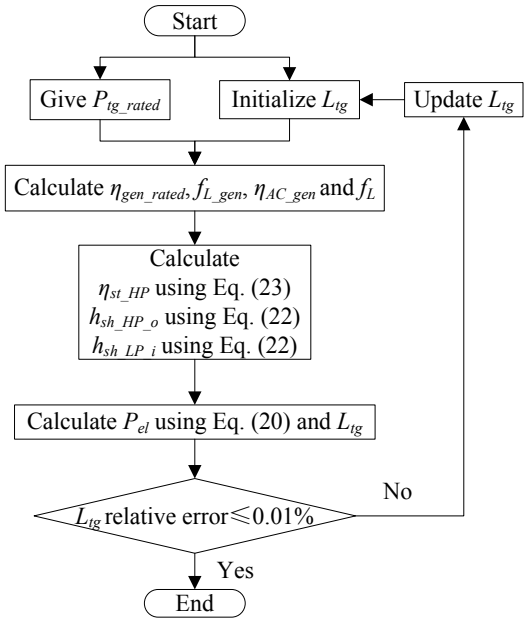

Figure A1. Flow chart for the calculation of turbo-generator produced electric power.

The thermal power transferred from the steam to the condenser cooling medium (usually seawater) is calculated by the following equation:

$$\dot{Q}_c = \dot{m}_c(\square_{s\square\_LP\_o} - \square_c) \tag{A24}$$

where the specific enthalpy of the superheated steam exiting the steam turbine LP stage, $h_{sh\_LP\_o}$, can be derived using a similar equation as the one used for the steam turbine HP stage (eq. (A22) and (A23)), and h_c is the specific enthalpy of the condensate water exiting the condenser. The mass flow rate of the condenser seawater pump is calculated by the following equation:

$$\dot{m}_{c\_sw} = \dot{Q}_c/(c_{p_{sw}}\Delta T_{sw}) \tag{A25}$$

where c_{p_sw} is the condenser seawater specific heat and ΔT_{sw} is the temperature increase of the seawater in the condenser.

Two pinch points exist in the dual pressure steam WHR system; one is at the section where the exhaust gas exits the LP superheater and the other one is at the boiler outlet section. The temperature differences at these pinch points are calculated by the following equations:

$$\Delta T_{pp\_HP} = T_{3g} - T_{s\_HP} \geq 10^o C \tag{A26}$$

$$\Delta T_{pp\_LP} = T_{5g} - T_{s\_LP} \geq 15^o C \tag{A27}$$

where T_{s_HP} and T_{s_LP} are the temperatures of the saturated water/steam in the HP and LP steam drum, respectively. Eq. (A26) and (A27) also indicate the minimum accepted values of the pinch point

temperature differences considered in this study as suggested by Ahmed et al. (2018).

The increase in the ship propulsion installation efficiency due to the electric power generation is calculated by using the following equation:

$$\Delta\eta_{el} = \left(P_{el} - \sum_{pumps} P\right)/\left(\dot{m}_f H_L\right) \quad \text{(A28)}$$

where $\dot{m}_f$ is the engine fuel mass flow rate and can be derived by using the exhaust gas mass flow rate and the air/fuel equivalence ratio, whereas H_L denotes the fuel lower heating value.

The WHR2 system model was developed in the MATLAB environment. The computational procedure flowchart is given in Fig. A2. The required input data include the engine exhaust gas mass flow rate, temperature, air/fuel equivalence ratio and the mass flow rate of saturated steam for the ship heating services as well as the WHR2 steam system pressures. The temperatures of the jacket cooling water and the compressor outlet air are also needed for the case of heating the feed water using the jacket water and air cooler. The initial value for the exhaust gas boiler outlet temperature is assumed to be 10°C higher than the sulphuric acid dew temperature point.

To start the calculation procedure, the following equation is used for the estimation of the HP superheated steam mass flow rate, which was derived from Equation (A18) considering the ideal Rankine cycle and ignoring the system pumps effects:

$$\dot{m}_{sh\_HP} = \frac{\dot{Q}_b - \dot{m}_{s\_hs}(h_{s\_HP} - h_{w\_LP})}{r_{sh\_LH}(h_{2sLP} - h_{w\_LP}) + (h_{3sHP} - h_{w\_LP})} \quad \text{(A29)}$$

The mass flow rates of the water/steam in various sections of the WHR system are derived by using the equations of Table A2 and the mass flow rate ratios values provided in Table 2. The derived mass flow rates of the water/steam and the pressure drops of the corresponding sections are used to calculate the pumps powers by employing Equation (A19). The specific enthalpies of the water/steam entering and exiting the E/G boiler sections are calculated considering the heat transferred via the boiler sections. The actual HP superheated steam mass flow rate is derived using Equation (A18), and the corresponding relative error is calculated and checked against the set convergence criterion (a relative percentage error of 0.01% was used in this study). The exhaust gas temperatures in the boiler sections are calculated by using the equations in Table A1, and subsequently, the two pinch points temperature differences (of the boiler HP and LP stages) are estimated and checked against and minimum accepted values. The parameters including the turbo-generator produced electric power and the steam cycle efficiency are calculated using Equations (A20) and (A28).

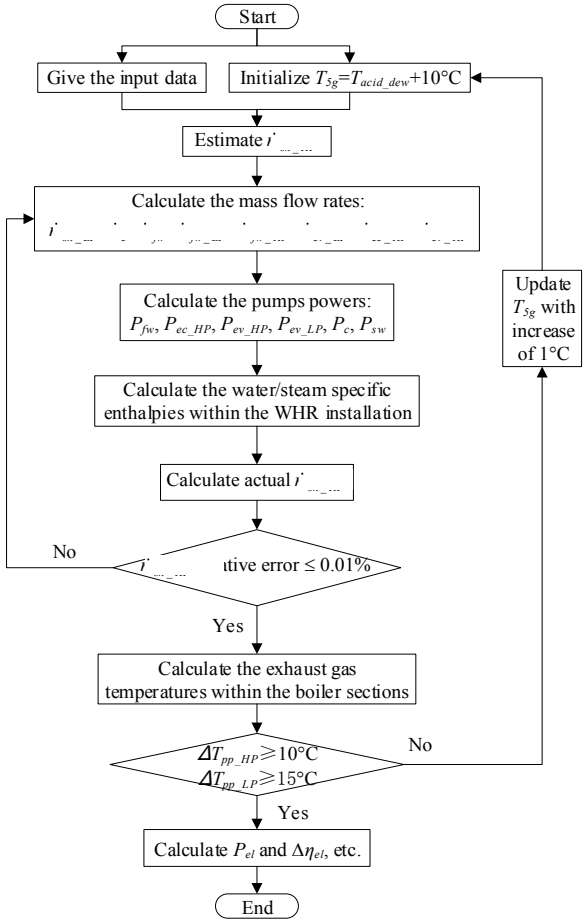

Figure A2. Flow chart of the dual pressure steam WHR system (WHR2) computational procedure.